Kaneko Y, Kitazato K, Basaki Y. (2004). Integrin-linked kinase regulates vascular morphogenesis induced by vascular endothelial growth factor. *J Cell Sci* **117**: 407–415.

Kohno K, Izumi H, Uchiumi T, Ashizuka M, Kuwano M. (2003). The pleiotropic functions of the Y-box-binding protein, YB-1. *Bioessays* **25**: 691–698.

Koike K, Uchiumi T, Ohga T, Toh S, Wada M, Kohno K *et al.* (1997). Nuclear translocation of the Y-box binding protein by ultraviolet irradiation. *FEBS Lett* **417**: 390–394.

Kryczek I, Lange A, Mottram P, Alvarez X, Cheng P, Hogan M *et al.* (2005). CXCL12 and vascular endothelial growth factor synergistically induce neoangiogenesis in human ovarian cancers. *Cancer Res* **65**: 465–472.

Kuwano M, Oda Y, Izumi H, Yang SJ, Uchiumi T, Iwamoto Y *et al.* (2004). The role of nuclear Y-box binding protein 1 as a global marker in drug resistance. *Mol Cancer Ther* **3**: 1485–1492.

Ladomery M, Sommerville J. (1995). A role for Y-box proteins in cell proliferation. *Bioessays* **17**: 9–11.

Maruyama Y, Ono M, Kawahara A, Yokoyama T, Basaki Y, Kage M *et al.* (2006). Tumor growth suppression in pancreatic cancer by a putative metastasis suppressor gene Cap43/NDRG1/Drg-1 through modulation of angiogenesis. *Cancer Res* **66**: 6233–6242.

Matsumoto K, Wolffe AP. (1998). Gene regulation by Y-box proteins: coupling control of transcription and translation. *Trends Cell Biol* **8**: 318–323.

Mossink MH, van Zon A, Scheper RJ, Sonneveld P, Wiemer EA. (2003). Vaults: a ribonucleoprotein particle involved in drug resistance? *Oncogene* **22**: 7458–7467.

Muller A, Homey B, Soto H, Ge N, Catron D, Buchanan ME *et al.* (2001). Involvement of chemokine receptors in breast cancer metastasis. *Nature* **410**: 50–56.

Murakami T, Maki W, Cardones AR, Fang H, Tun Kyi A, Nestle FO *et al.* (2002). Expression of CXC chemokine receptor-4 enhances the pulmonary metastatic potential of murine B16 melanoma cells. *Cancer Res* **62**: 7328–7334.

Ohga T, Koike K, Ono M, Makino Y, Itagaki Y, Tanimoto M *et al.* (1996). Role of the human Y box-binding protein YB-1 in cellular sensitivity to the DNA-damaging agents cisplatin, mitomycin C, and ultraviolet light. *Cancer Res* **56**: 4224–4228.

Ohga T, Uchiumi T, Makino Y, Koike K, Wada M, Kuwano M *et al.* (1998). Direct involvement of the Y-box binding protein YB-1 in genotoxic stress-induced activation of the human multidrug resistance 1 gene. *J Biol Chem* **273**: 5997–6000.

Porcile C, Bajetto A, Barbieri F, Barbero S, Bonavia R, Biglieri M *et al.* (2005). Stromal cell-derived factor-1alpha (SDF-1alpha/CXCL12) stimulates ovarian cancer cell growth through the EGF receptor transactivation. *Exp Cell Res* **308**: 241–253.

Robledo MM, Bartolome RA, Longo N, Rodriguez-Frade JM, Mellado M, Longo I *et al.* (2001). Expression of functional chemokine receptors CXCR3 and CXCR4 on human melanoma cells. *J Biol Chem* **276**: 45098–45105.

Scotton CJ, Wilson JL, Milliken D, Stamp G, Balkwill FR. (2001). Epithelial cancer cell migration: a role for chemokine receptors? *Cancer Res* **61**: 4961–4965.

Scotton CJ, Wilson JL, Scott K, Stamp G, Wilbanks GD, Fricker S *et al.* (2002). Multiple actions of the chemokine CXCL12 on epithelial tumor cells in human ovarian cancer. *Cancer Res* **62**: 5930–5938.

Sorokin AV, Selyutina AA, Skabkin MA, Guryanov SG, Nazimov IV, Richard C *et al.* (2005). Proteasome-mediated cleavage of the Y-box-binding protein 1 is linked to DNA-damage stress response. *EMBO J* **24**: 3602–3612.

Stein U, Bergmann S, Scheffer GL, Scheper RJ, Royer HD, Schlag PM *et al.* (2005). YB-1 facilitates basal and 5-fluorouracil-inducible expression of the human major vault protein (MVP) gene. *Oncogene* **24**: 3606–3618.

Stein U, Jurchott K, Walther W, Bergmann S, Schlag PM, Royer HD. (2001). Hyperthermia-induced nuclear translocation of transcription factor YB-1 leads to enhanced expression of multidrug resistance-related ABC transporters. *J Biol Chem* **276**: 28562–28569.

Stenina OI, Poptic EJ, DiCorleto PE. (2000). Thrombin activates a Y box-binding protein (DNA-binding protein B) in endothelial cells. *J Clin Invest* **106**: 579–587.

Sutherland BW, Kucab J, Wu J, Lee C, Cheang MC, Yorida E *et al.* (2005). Akt phosphorylates the Y-box binding protein 1 at Ser102 located in the cold shock domain and affects the anchorage-independent growth of breast cancer cells. *Oncogene* **24**: 4281–4292.

Supplementary Information accompanies the paper on the Oncogene website (http://www.nature.com/onc).

Bioorganic & Medicinal Chemistry Letters 19 (2009) 3863–3865

Contents lists available at ScienceDirect

Bioorganic & Medicinal Chemistry Letters

journal homepage: www.elsevier.com/locate/bmcl

Total synthesis and determination of the absolute configuration of FD-838, a naturally occurring azaspirobicyclic product

Yujiro Hayashi [a,b,*], Kuppusamy Sankar [a], Hayato Ishikawa [a], Yuriko Nozawa [c], Kazutoshi Mizoue [c], Hideaki Kakeya [d]

[a] Department of Industrial Chemistry, Faculty of Engineering, Tokyo University of Science, Kagurazaka, Shinjuku-ku, Tokyo 162-8601, Japan
[b] Research Institute for Science and Technology, Tokyo University of Science, Kagurazaka, Shinjuku-ku, Tokyo 162-8601, Japan
[c] Research Center of Taisho Pharmaceutical Co., Ltd, 1-403, Yoshino-cho, Kita-ku, Saitama-shi, Saitama 331-9530, Japan
[d] Department of System Chemotherapy and Molecular Sciences, Graduate School of Pharmaceutical Sciences, Kyoto University, Sakyo-ku, Kyoto 606-8501, Japan

ARTICLE INFO

Article history:
Received 5 March 2009
Revised 27 March 2009
Accepted 30 March 2009
Available online 5 April 2009

Keywords:
FD-838
Total synthesis
Absolute configuration

ABSTRACT

The first asymmetric total synthesis of FD-838, a naturally occurring azaspirobicyclic product, has been accomplished allowing determination of its absolute stereochemistry.

Pseurotins,[1] synerazol,[2] and azaspirene[3] are natural products possessing a unique azaspirocyclic framework, such as the 1-oxa-7-azaspiro[4.4]non-2-ene-4,6-dione ring system (Fig. 1). The pseurotins are a small family of secondary microbial metabolites isolated from a culture broth of *Pseudeurotium ovalis* (strain S2269/F) in 1976 by Bloch et al.[1a] Pseurotin A was reported to inhibit chitin synthase by Sterner and co-workers in 1993,[1e] and was also found to induce cell differentiation of PC12 cells by Komagata et al. in 1995.[1f] The structure of pseurotin A, including its absolute stereochemistry, has been unambiguously determined by a single-crystal X-ray analysis of its 12,13-dibromo derivative.[1b] Synerazol, an antifungal antibiotic isolated by Ando and co-workers in 1991 from the culture broth of *Aspergillus fumigatus* SANK 10588, is active against *Candida albicans* and other fungi, showing marked synergistic activity with azole-type antifungal agents.[2] Azaspirene, isolated from the fungus *Neosartorya* sp. by Kakeya and co-workers was found not only to inhibit the endothelial migration induced by vascular endothelial growth factor,[3] but also to exhibit antiangiogenic effects by blocking Raf-1 activation.[4] These compounds possess the same highly oxygenated azaspiro core structure with different side chains. Because of its unique structure and interesting biological properties, there have been several attempts at its total synthesis.[5] Our group has accomplished the first enantioselective total synthesis of pseurotin A,[6] F2,[6] synerazol,[7] and azaspirene,[8] in which the aldol chemistry of a chiral benzylidene lactam with an appropriate aldehyde, followed by successive oxidation and dehydration, creates the key azaspiro structure (Eq. 1). By these syntheses, the absolute configurations of synerazol[9] and azaspirene have been determined. Tadano and co-workers also reported the total syntheses of pseurotin A, F2, and azaspirene from D-glucose.[10]

FD-838, isolated from *A. fumigatus fresenius* F-838 by Mizoue and co-workers of Taisho pharmaceutical company in 1985, is reported to induce the differentiation of leukemia in cultures and to inhibit the growth of certain Gram-positive bacteria and fungi.[11] Recently, Rovis and Orellana reported the synthesis of the spirobicyclic core of FD-838 via the asymmetric Stetter reaction.[12] Its total synthesis has not been accomplished, and its absolute configuration has been unknown, with its optical rotation being reported to be zero ($[\alpha]_D^{26}$ 0 (*c* 0.1, MeOH)).[10] As the fungus no longer produces FD-838, chemical synthesis is the only way to obtain this molecule. Despite the interesting biological properties, biological investigations cannot be performed because of lack of supply of FD-838.

Despite the structural similarity of FD-838, pseurotin A, synerazol, and azaspirene, the reported biological properties of these natural products are rather different, as described above. Systematic comparison of the biological properties of these natural products and their derivatives is highly desirable, and a sufficient quantity of not only the natural products but also several

* Corresponding author.
E-mail address: hayashi@ci.kagu.tus.ac.jp (Y. Hayashi).

0960-894X/$ - see front matter © 2009 Elsevier Ltd. All rights reserved.
doi:10.1016/j.bmcl.2009.03.154

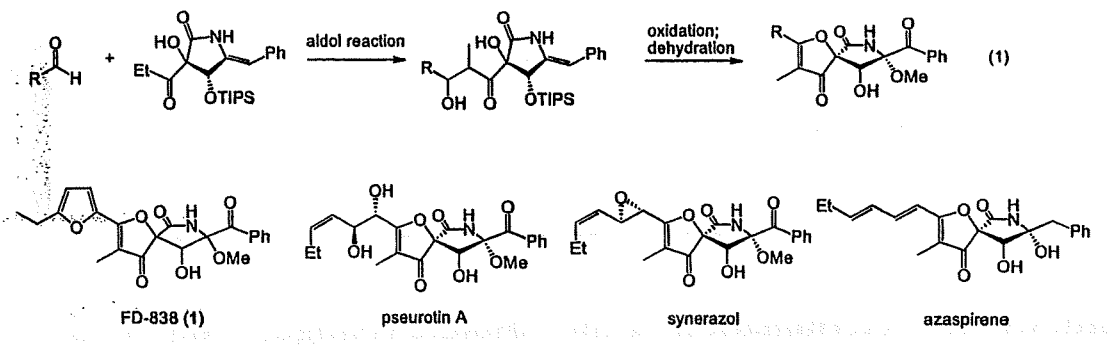

Figure 1. FD-838 (**1**), pseurotin A, synerazol, and azaspirene.

derivatives is required for such biological studies. Because we had established a synthetic method for the latter three natural products, we began to investigate the total synthesis of FD-838. In this communication we report the first total synthesis of FD-838 along with the determination of its absolute configuration.

Because we have already established the synthesis of the azaspirocyclic framework, the same synthetic strategy would be applicable to the synthesis of FD-838. The aldol reaction between 5-ethyl-2-formylfuran and the functionalized benzylidene lactam **2**, which was a key intermediate for other azaspiro compounds prepared from methyl pentenoate via Sharpless dihydroxylation as a key step, was examined.[6–8] The lithium enolate of **2** reacted with 5-ethyl-2-formylfuran, affording the desired aldol product **3** (mixture of four diastereomers, 1:1:3:3.5) in 40% yield with recovery of the lactam **2** in 49% yield (78% yield based on the recovered starting material (br sm)). Oxidation of the alcohol **3** with Dess–Martin periodinane (DMP)[13] in CH_2Cl_2 in the presence of $NaHCO_3$ afforded the 1,3-diketone **5**. When 1,3-diketone **5** was treated with silica gel on TLC, cyclization followed by dehydration proceeded because of the acidity of the silica gel to produce azaspiro derivative **4** in 20% yield with recovery of 1,3-diketone **5** in 37% yield over two steps. Recovered 1,3-diketone **5** was further transformed into azaspiro derivative **4** in 27% yield (54% br sm) by the same reaction conditions. Oxidation of the benzylidene moiety with dimethyldioxirane (DMD)[14] in MeOH afforded a mixture of methoxy derivative **6** and hydroxy derivative **7** in 56% yield (single diastereomers at the benzylic alcohol position), the mixture of which was treated with DMP in CH_2Cl_2 to provide benzoylated methoxy **8** and hydroxy **9** derivatives in 49% and 16% yields, respectively, which can be separated by TLC. Removal of the TIPS group with NH_4F in MeOH afforded FD-838 (**1**) in 62% yield (89%, br sm). Synthetic FD-838 exhibited identical properties to those of the natural substance (^1H NMR, ^{13}C NMR, IR).

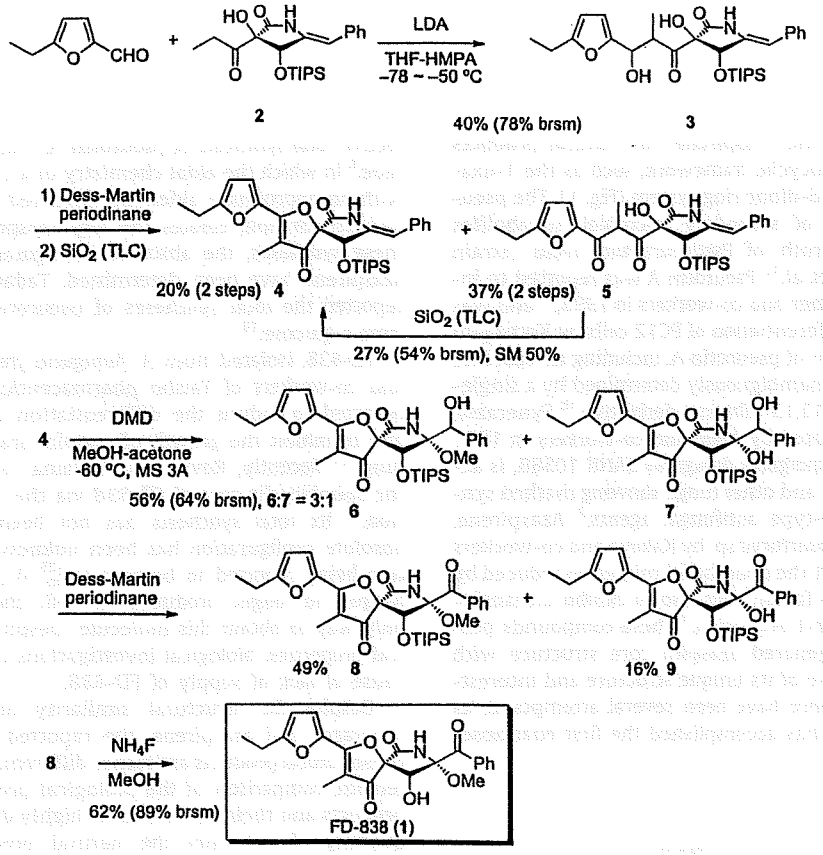

Scheme 1. The synthesis of FD-838.

Because the optical rotation of natural FD-838 was reported to be zero using MeOH as a solvent,[11] the optical rotation was measured in other solvents, such as $CHCl_3$. The optical rotations of natural FD-838 and synthetic FD-838 show large negative values (synthetic FD-838: $[\alpha]_D^{26}$ −41.9 (*c* 0.4, $CHCl_3$), natural FD-838: $[\alpha]_D^{26}$ −32.4 (*c* 0.7, $CHCl_3$)), indicating that both compounds have the same absolute configuration.[15] Thus, the absolute configuration is determined, as shown in Scheme 1.

In summary, we have accomplished the first asymmetric total synthesis of FD-838 along with the determination of its absolute configuration.

Acknowledgment

This work was supported by a Grant-in Aid for Scientific Research from the Ministry of Education, Culture, Sports, Science and Technology, Government of Japan.

Supplementary data

Supplementary data associated with this article can be found, in the online version, at doi:10.1016/j.bmcl.2009.03.154.

References and notes

1. (a) Bloch, P.; Tamm, C.; Bollinger, P.; Petcher, T. J.; Weber, H. P. *Helv. Chim. Acta* **1976**, *59*, 133; (b) Weber, H. P.; Petcher, T. J.; Bloch, P.; Tamm, C. *Helv. Chim. Acta* **1976**, *59*, 137; (c) Bloch, P.; Tamm, C. *Helv. Chim. Acta* **1981**, *64*, 304; (d) Breitenstein, W.; Chexal, K. K.; Mohr, P.; Tamm, C. *Helv. Chim. Acta* **1981**, *64*, 379; (e) Wenke, J.; Anke, H.; Sterner, O. *Biosci., Biotechnol., Biochem.* **1993**, *57*, 961; (f) Komagata, D.; Fujita, S.; Yamashita, N.; Saito, S.; Morino, T. *J. Antibiot.* **1996**, *49*, 958.
2. Ando, O.; Satake, H.; Nakajina, M.; Sato, A.; Nakamura, T.; Kinoshita, T.; Furuya, K.; Haneishi, T. *J. Antibiot.* **1991**, *44*, 382.
3. Asami, Y.; Kakeya, H.; Onose, R.; Yoshida, A.; Matsuzaki, H.; Osada, H. *Org. Lett.* **2002**, *4*, 2845.
4. Asami, Y.; Kakeya, H.; Komi, Y.; Kojima, S.; Nishikawa, K.; Beebe, K.; Neckers, L.; Osada, H. *Cancer Sci.* **2008**, *99*, 1853.
5. Synthetic studies of pseurotin A; see: (a) Dolder, M.; Shao, X.; Tamm, C. *Helv. Chim. Acta* **1990**, *73*, 63; (b) Shao, X.; Dolder, M.; Tamm, C. *Helv. Chim. Acta* **1990**, *73*, 483; (c) Su, Z.; Tamm, C. *Helv. Chim. Acta* **1995**, *78*, 1278; (d) Su, Z.; Tamm, C. *Tetrahedron* **1995**, *51*, 11177; (e) Mitchell, J. M.; Finney, N. S. *Org. Biomol. Chem.* **2005**, *3*, 4274; Biosynthetic study, see: (f) Igarashi, Y.; Yabuta, Y.; Sekine, A.; Fujii, K.; Harada, K.; Oikawa, T.; Sato, M.; Furumai, T.; Oki, T. *J. Antibiot.* **2004**, *57*, 748.
6. Hayashi, Y.; Shoji, M.; Yamaguchi, S.; Mukaiyama, T.; Yamaguchi, J.; Kakeya, H.; Osada, H. *Org. Lett.* **2003**, *5*, 2287.
7. Hayashi, Y.; Shoji, M.; Mukaiyama, T.; Gotoh, H.; Yamaguchi, S.; Nakata, M.; Kakeya, H.; Osada, H. *J. Org. Chem.* **2005**, *70*, 5643.
8. Hayashi, Y.; Shoji, M.; Yamaguchi, J.; Sato, K.; Yamaguchi, S.; Mukaiyama, T.; Sakai, K.; Asami, Y.; Kakeya, H.; Osada, H. *J. Am. Chem. Soc.* **2002**, *124*, 12078.
9. Igarashi and co-workers also determined the absolute configuration of synerazol using modified MTPA method, see: Igarashi, Y.; Yabuta, Y.; Furumai, T. *J. Antibiot.* **2004**, *57*, 537.
10. (a) Aoki, S.; Ohi, T.; Shimizu, K.; Shiraki, R.; Takao, K.; Tadano, K. *Heterocycles* **2004**, *62*, 161; (b) Aoki, S.; Ohi, T.; Shimizu, K.; Shiraki, R.; Takao, K.; Tadano, K. *Bull. Chem. Soc. Jpn.* **2004**, *77*, 1703; Review, see: (c) Takao, K.; Aoki, S.; Tadano, K. *J. Syn. Org. Chem. Jpn.* **2007**, *65*, 460.
11. Mizoue, K.; Okazaki, T.; Hanada, K.; Amamoto, T.; Yamagishi, M.; Omura, S. Eur. Pat. Appl. EP 216607, J P Appl. 205278; *Chem. Abstr.*, **1987**, *107*, 132627x.
12. Orellana, A.; Rovis, T. *Chem. Commun.* **2008**, 730.
13. (a) Dess, D. B.; Martin, J. C. *J. Org. Chem.* **1983**, *48*, 4155; (b) Dess, D. B.; Martin, J. C. *J. Am. Chem. Soc.* **1991**, *113*, 7277; (c) Ireland, R. E.; Liu, L. *J. Org. Chem.* **1993**, *58*, 2899; (d) Meyer, S. D.; Schreiber, S. L. *J. Org. Chem.* **1994**, *59*, 7549.
14. (a) Adam, W.; Bialas, J.; Hadjiarapoglou, L. *Chem. Ber.* **1991**, *124*, 2377; (b) Koseki, Y.; Kusano, S.; Ichi, D.; Yoshida, K.; Nagasaka, T. *Tetrahedron* **2000**, *56*, 8855.
15. A small quantity of the natural FD-838 would cause the inconsistency of the optical rotation.

CHEMBIOCHEM

DOI: 10.1002/cbic.200800787

Identification of Cytochrome P450s Required for Fumitremorgin Biosynthesis in *Aspergillus fumigatus*

Naoki Kato,[a] Hirokazu Suzuki,[a, d] Hiroshi Takagi,[a] Yukihiro Asami,[a, e] Hideaki Kakeya,[a, f] Masakazu Uramoto,[a] Takeo Usui,[b] Shunji Takahashi,[a] Yoshikazu Sugimoto,[c] and Hiroyuki Osada*[a]

Fumitremorgin C, a diketopiperazine mycotoxin produced by *Aspergillus fumigatus*, is a potent and specific inhibitor of breast cancer resistance protein (BCRP). Elucidation of the fumitremorgin C biosynthetic pathway provides a strategy for new drug design. A structure–activity relationship study based on metabolites related to the *ftm* gene cluster revealed that the process most crucial for inhibitory activity against BCRP was cyclization to form fumitremorgin C. To determine the gene involved in the cyclization reaction, targeted gene inactivation was performed with candidate genes in the *ftm* cluster. Analysis of the gene disruptants allowed us to identify *ftmE*, one of the cytochrome P450 genes in the cluster, as the gene responsible for the key step in fumitremorgin biosynthesis. Additionally, we demonstrated that the other two cytochrome P450 genes, *ftmC* and *ftmG*, were involved in hydroxylation of the indole ring and successive hydroxylation of fumitremorgin C, respectively.

Introduction

Breast cancer resistance protein (BCRP) is a member of the multidrug transporters of the ATP-binding cassette family, which can actively extrude a wide range of structurally diverse drugs, toxins, endogenous compounds, and their metabolites across the plasma membranes of cells.[1,2] Although these ATP-dependent efflux pumps were once thought to be of relevance only to multidrug resistance in cancer cells, it is now clear that they have a pronounced role in the pharmacokinetics of a broad range of drugs and toxins. It is noteworthy that recent findings have revealed intriguing roles for BCRP in stem cells.[2,3] Specific inhibitors are therefore required for further understanding of the pharmacological and physiological roles of this interesting transporter in normal and malignant stem cells, as well as of clinical applications of BCRP inhibition in cancer chemotherapy. Two BCRP inhibitors—GF120918 and fumitremorgin C (**6**)—have been well characterized. GF120918 is a synthetic product originally developed as a P-glycoprotein inhibitor.[4,5] In contrast, compound **6**, a diketopiperazine mycotoxin produced by *Aspergillus fumigatus*,[6] is capable of completely reversing mitoxantrone, doxorubicin, and topotecan resistance in BCRP-overexpressing cells but does not reverse resistance to cells that overexpress other multidrug transporters such as P-glycoprotein or multidrug-resistant protein 1.[7,8] Several synthetic analogues of **6** have been investigated and one such, Ko143, showed more potent inhibitory effects as well as lower in vivo toxicity.[9,10] This indicates that **6** may serve as a lead compound for more potent and specific BCRP inhibitors. Elucidation of the fumitremorgin biosynthetic pathway provides a strategy for new drug design.

The *A. fumigatus* genome harbors more than 20 biosynthetic gene clusters for secondary metabolites.[11] Their gene organization allows us to predict biosynthetic products that arise from the corresponding gene clusters. It has been suggested that some of the gene clusters are involved in the biosynthesis of known fungal metabolites.[12–14] The *ftm* gene cluster has also been investigated as the most probable candidate for the biosynthesis of **6** and its related compounds.[15–17] It apparently consists of nine genes (Figure 1 A). A genetic study has indicated that the dimodular nonribosomal peptide synthetase (NRPS) gene *ftmA* encodes brevianamide F synthetase.[17] Func-

[a] *Dr. N. Kato,[+] Dr. H. Suzuki,[+] H. Takagi, Dr. Y. Asami, Dr. H. Kakeya, Dr. M. Uramoto, Dr. S. Takahashi, Dr. H. Osada*
Chemical Biology Department, Advanced Science Institute, RIKEN
Wako, Saitama 351-0198 (Japan)
Fax: (+81) 48-462-4669
E-mail: hisyo@riken.jp

[b] *Dr. T. Usui*
Graduate School of Life and Environmental Sciences, University of Tsukuba
Ibaraki 305-8572 (Japan)

[c] *Dr. Y. Sugimoto*
Division of Chemotherapy, Faculty of Pharmacy, Keio University
Tokyo 105-8512 (Japan)

[d] *Dr. H. Suzuki[+]*
Present address: Organization of Advanced Science and Technology
Kobe University
Hyogo 657-8501 (Japan)

[e] *Dr. Y. Asami*
Present address: Graduate School of Pharmaceutical Sciences
The University of Tokyo
Tokyo 113-0033 (Japan)

[f] *Dr. H. Kakeya*
Present address: Division of Bioinformatics and Chemical Genomics
Graduate School of Pharmaceutical Sciences, Kyoto University
Kyoto 606-8501 (Japan)

[+] *These authors contributed equally to this work.*

Supporting information for this article is available on the WWW under http://dx.doi.org/10.1002/cbic.200800787.

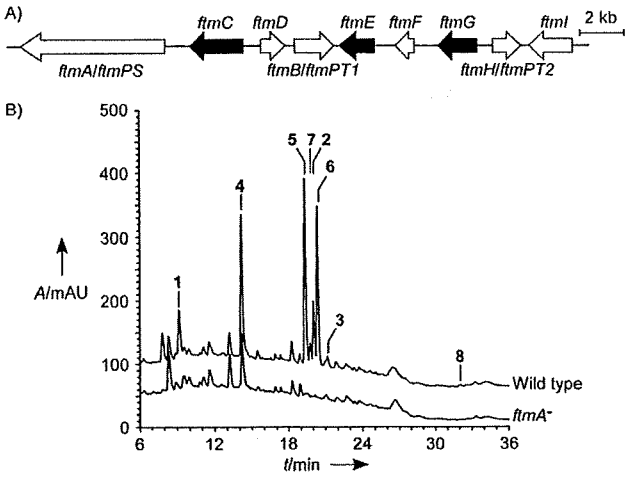

Figure 1. The production of metabolites associated with the *ftm* cluster in *A. fumigatus*. A) Gene organization of the *ftm* cluster. The three cytochrome P450 genes are indicated in black. The genes shown in gray—*ftmA/ftmPS*, *ftmB/ftmPT1*, and *ftmH/ftmPT2*—encode a dimodular NRPS[17] and prenyltransferases.[15,16] B) HPLC chromatograms of culture extracts of the wild-type and the *ftmA*⁻ strains derived from *A. fumigatus* BM939. UV detection was carried out at 220 nm. Retention times of authentic standards of fumitremorgins are denoted by Arabic numerals. MS analysis confirmed that the peak at a retention time of 14.5 min in the chromatograms of extracts of the *ftmA*⁻ strains contained no compound **4**.

tional analyses of FtmB and FtmH (also termed FtmPT1 and FtmPT2, respectively) have been performed to characterize their enzymatic activities.[15,16] These results have suggested that this gene cluster directs the biosynthesis of fumitremorgin B (**8**), with *ftmA*, *ftmB*, and *ftmH* involved in the first, second, and last steps, respectively, in the biosynthetic pathway to **8**. However, the functions of the other *ftm* genes remain to be elucidated. Lack of fumitremorgin production in the genome reference strain Af293[17] makes a full understanding of the cluster difficult, so in exploring the fumitremorgin pathway we utilized the strain BM939, which is a high producer of **6** and its related compounds.[18]

In the work reported here we carried out a structure–activity relationship (SAR) study, revealing that the most crucial event for exertion of inhibitory activity against BCRP was the C–N bond formation in the synthesis of **6**. To identify the gene responsible for the key step to form **6**, targeted gene inactivation for candidate genes in the *ftm* cluster was performed. Analysis of the knockout mutants allowed us to identify the cytochrome P450 gene *ftmE* as involved in the C–N bond formation. In addition, we demonstrated the role of the other two cytochrome P450 genes—*ftmC* and *ftmG*—in the fumitremorgin pathway.

Results and Discussion

Structure–activity relationship study based on metabolites related to the *ftm* cluster

To examine the biological activities of **6** and its related compounds, we isolated metabolites associated with the *ftm* cluster from BM939, a fumitremorgin-producing strain of *A. fumigatus*. Eight diketopiperazine compounds—brevianamide F (**1**),

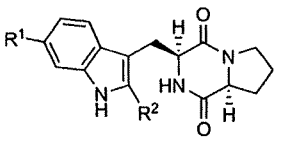

brevianamide F (**1**, R^1=H, R^2=H)
tryprostatin B (**2**, R^1=H, R^2=dimethylallyl)
desmethyltryprostatin A (**4**, R^1=OH, R^2=dimethylallyl)
tryprostatin A (**5**, R^1=OMe, R^2=dimethylallyl)

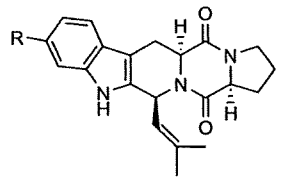

demethoxyfumitremorgin C (**3**, R=H)
fumitremorgin C (**6**, R=OMe)

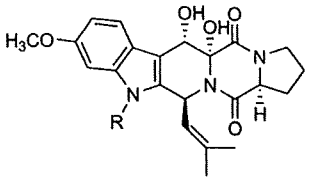

12α,13α-dihydroxyfumitremorgin C (**7**, R=H)
fumitremorgin B (**8**, R=dimethylallyl)

tryprostatin B (**2**), demethoxyfumitremorgin C (**3**), desmethyltryprostatin A (**4**), tryprostatin A (**5**), fumitremorgin C (**6**), 12α,13α-dihydroxyfumitremorgin C (**7**), and fumitremorgin B (**8**)—were prepared, and their structures were determined by mass spectrometry and NMR analysis. Compound **4**, a desmethyl analogue of **5**, is a new compound. Disruption of *ftmA* in the BM939 strain caused a deficiency in the production of **1**–**8** (Figure 1B), indicating that these metabolites are products of the *ftm* cluster

These metabolites share a diketopiperazine scaffold but are structurally diverse and thereby useful for SAR studies of their bioactivities. In fact, evaluation of **1**–**8** with regard to BCRP inhibitory activity (Figure 2A and B) revealed that **6** was the most potent inhibitor out of all of the derivatives tested. The SAR study also indicates that the following three moieties were important for the inhibitory activity of **6** against BCRP (Figure 2C). 1) The most crucial moiety involved in the activity of **6** is the covalent bond between C-3 and N-4, because compounds **3** and **6**–**8** all showed detectable activities in assays in vivo and in vitro, whereas the activities of **1**, **2**, **4**, and **5** were negligible. Although compound **5** has been reported as a BCRP inhibitor,[19] its activity was much lower than that of **6** under the conditions used in this study. 2) Dihydroxylation at C-12 and C-13 of **6** impaired inhibitory activity at the cellular level. Reversal effects of **1**–**6**, but not of **7** or **8**, on drug resist-

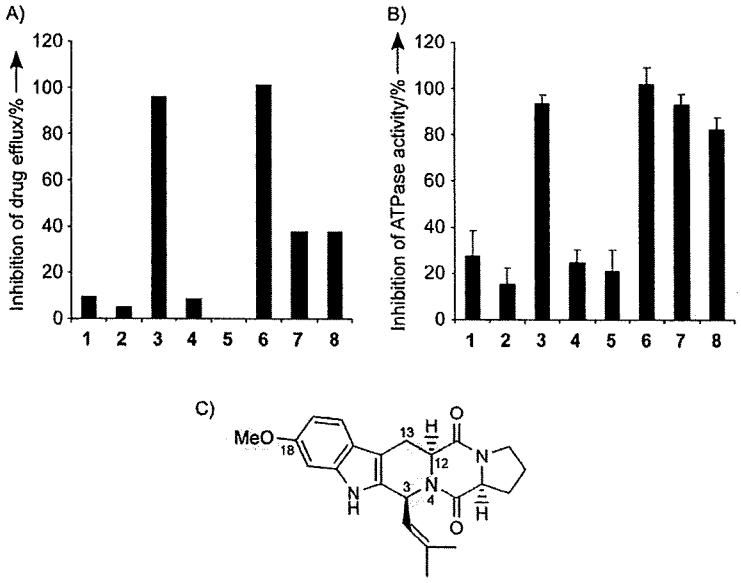

Figure 2. Evaluation of BCRP inhibitory effects of fumitremorgins. A) Inhibition of drug efflux in K562/BCRP cells by fumitremorgins **1**–**8**. IC_{50} values of growth inhibition of K562/BCRP cells by SN-38 in the presence of fumitremorgins (3 μM) were determined. IC_{50} values in K562/BCRP and K562 cells (parental cells) without fumitremorgins were defined as 0 and 100% inhibition, respectively. B) Inhibition of BCRP-dependent ATPase activity by fumitremorgins **1**–**8**. The vanadate-sensitive ATPase activities in the presence of fumitremorgins (50 μM) were measured in vitro with use of BCRP membranes (BD Biosciences). C) SAR of fumitremorgins. Of the moieties shown in gray, the covalent bond between C-3 and N-4 and the methoxy group at C-18 are important for the inhibitory activity of **6** against BCRP, whereas dihydroxylation at C-12 and C-13 of **6** affects the activity at the cellular level.

ance in BCRP-overexpressing K562 cells was in good agreement with their inhibitory activities against BCRP-dependent ATPase activities. A possible explanation for the weaker effects of **7** and **8** in the in vivo assay is a change in membrane permeability due to further modifications. 3) Compound **6** showed clear inhibitory activities even at submicromolar concentrations, whereas its demethoxy form **3** did not (data not shown), which suggests that the methoxy group at C-18 is important, in agreement with previous suggestions.[9]

Although fumitremorgins are harmful tremorgenic mycotoxins produced by *A. fumigatus* and related fungi,[6] some of the biosynthetic intermediates besides the BCRP inhibitor **6** have been shown to have interesting biological and pharmacological activities.[18,20] Recently, Jain et al. reported that **5**, which has inhibitory effects on the cell cycle[18] and microtubule assembly,[21] and its synthetic derivatives showed insignificant bioactivities.[22] Consistently with this, such inhibitory effects were not detectable in the compounds isolated in this study.

Identification of the key enzymes for fumitremorgin biosynthesis

The SAR study of fumitremorgins **1**–**8** revealed the important moieties involved in exertion of the BCRP inhibitory activity of **6**. From this information we tried to identify the genes involved in the formation of such important moieties. None of the enzymes catalyzing the cyclization to form **6**, the subsequent hydroxylation at C-12 and C-13 of **6**, or the hydroxylation at C-6 of the indole ring had been previously identified. To identify the genes responsible for these reactions, we first cloned the *ftm* cluster from the strain BM939. A 27 kb DNA fragment that covered the *ftm* cluster of strain BM939 was sequenced, revealing that the cluster is extremely similar to that of Af293 and consists of nine genes (see Table 1 for features of the *ftm* gene products). There were six uncharacterized genes in the *ftm* cluster. FtmC,

Table 1. Features of the *ftm* gene products of *A. fumigatus* BM939.

Protein	Size bp/aa	exon	Function[a]	Relatives[b] (identity/similarity [%])	Accession number
FtmA	6636/2211	1–6636	dimodular NRPS	nonribosomal peptide synthetase XyNRPSA from *Xylaria* sp. BCC 1067 (37/55)	ABF29402
FtmC	1955/559	1–969, 1033–1154, 1227–1525, 1597–1698, 1768–1955	cytochrome P450	isotrichodermin C-15 hydroxylase TRI11 from *Fusarium sporotrichioides* (31/46)	O13317
FtmD	1114/342	1–528, 614–1114	methyltransferase	cercosporin toxin biosynthesis protein CTB3 from *Cercospora nicotianae* (31/51)	ABC79591
FtmB	1464/464	1–1262, 1332–1464	prenyltransferase	dimethylallyltryptophan synthase DmaW from *Claviceps purpurea* (34/56)	AAP81210
FtmE	1581/526	1–1581	cytochrome P450	cytochrome P450 ELN2 from *Coprinopsis cinerea* (26/44)	BAA33717
FtmF	876/291	1–876	α-KG dioxygenase	fumonisin C-5 hydroxylase Fum3p/FUM9 from *Gibberella moniliformis* (29/48)	AAG27131
FtmG	1813/504	1–207, 273–389, 451–550, 604–672, 723–1313, 1383–1813	cytochrome P450	GA14-synthase P450-1 from *G. fujikuroi* (37/56)	CAA75565
FtmH	1349/427	1–1181, 1247–1349	prenyltransferase	tryptophan dimethylallyltransferase FgaPT2 from *A. fumigatus* (37/56)	AAX08549
FtmI	2043/680	1–2043	protein–protein interaction	ankyrin 1 isoform 2 from *Homo sapiens* (35/53)	NP_065210

[a] Functions of FtmD, FtmF, and FtmI were predicted on the basis of sequence similarities to known proteins. α-KG: α-ketoglutarate. [b] The listed homologous proteins exclude putative proteins derived from genomic projects.

FtmE, and FtmG show similarity to cytochrome P450s of filamentous fungi, while FtmF has similarity to proteins that belong to the α-ketoglutarate dioxygenase family.[23] These enzymes could have roles in the cyclization as well as in the hydroxylations. Besides the oxygenases, FtmD is predicted to function as an *O*-methyltransferase and is thus implicated in the methylation of the new intermediate **4** to give **5**. The *ftmI* gene encodes an ankyrin-repeat protein.[24]

To assign the roles of the oxygenase genes in fumitremorgin biosynthesis, we generated gene disruptants by replacing the entire coding region of each gene with the hygromycin B-resistance gene cassette (Δ*ftm*::*hph*; Figure 3). The *akuA*$^-$ strain (TAFK1.39), derived from BM939, was used as a host strain for the knockout experiments, and correct disruption events occurred in almost all hygromycin-resistant transformants (data not shown). Two to four transformants of each *ftm* disruption were cultivated for analysis of fumitremorgin production. The metabolite profiles of the disruptants—*ftmC*$^-$, *ftmE*$^-$, *ftmF*$^-$, and *ftmG*$^-$—were determined by HPLC and LC/ESI-MS (see Table S1 in the Supporting Information for productivity of fumitremorgins in the disruptants).

The disruption of *ftmC* led to substantial accumulation of **2** and its cyclization product **3** (Figure 4A). Compound **4** (the product hydroxylated at C-6 of the indole ring of **2**) and its downstream methoxy-group-containing metabolites **5**–**8** were not detected in the culture extracts of the *ftmC*$^-$ strain. The *ftmE* disruptants produced **2** and **5** but not their cyclization products **3** and **6** (Figure 4B). The disruption of *ftmG* resulted in the loss of production of **7** and **8** (Figure 4C). The production of **6** was observed in the *ftmG*$^-$ strain, indicating that hydroxylation of the indole ring and cyclization proceeded normally in this strain. These results clearly suggest the roles of the three cytochrome P450 genes in the fumitremorgin pathway: hydroxylation at C-6 of the indole ring, C–N bond formation to form **6**, and the subsequent dihydroxylation are mediated by *ftmC*, *ftmE*, and *ftmG*, respectively. On the other hand, the disruption of *ftmF* had no significant effect on the production of **1**–**8**, suggesting that *ftmF* should not be involved in their biosynthesis (data not shown).

On the basis of the phenotypes of the *ftm* disruptants, the functions of the three cytochrome P450 genes were demonstrated by use of a yeast expression system. The cytochrome P450 genes *ftmC*, *ftmE*, and *ftmG* were expressed in *Saccharomyces cerevisiae* with a P450 reduction partner gene of *A. fumigatus*, *AFUA_2g07940*. Microsomes that were prepared from *ftmC*-expressing yeast catalyzed the hydroxylation of **2** to

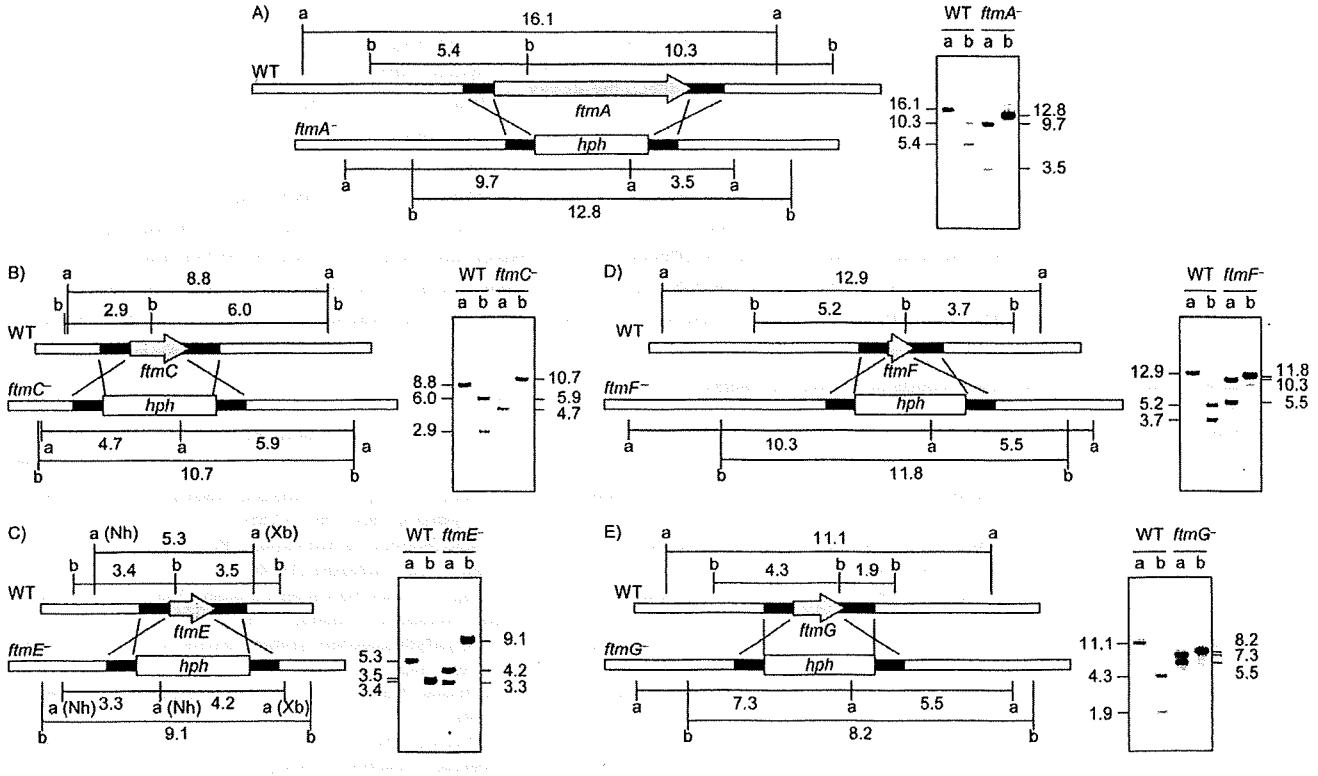

Figure 3. Construction of the *ftm* disruptants. DNA fragments (5.9 kb) containing 1 kb upstream and 1 kb downstream regions of the *ftm* genes and the hygromycin B-resistance cassette (*hph*) were used for the transformation of the wild-type strain (WT, TAFK1.39) and as probes for Southern hybridization. A) *ftmA* disruption: total DNA (10 μg) isolated from the hygromycin B-resistant transformants was digested with a) MluI, or b) ApaI. The WT strain shows a) 16.1, and b) 10.3 and 5.4 kb bands, whereas the *ftmA*$^-$ mutant shows a) 9.7 and 3.5, and b) 12.8 kb bands. B) *ftmC* disruption: total DNA was digested with a) NdeI, or b) Aor51HI. WT shows a) 8.8, and b) 6.0 and 2.9 kb bands, whereas the mutant shows a) 5.9 and 4.7, and b) 10.7 kb bands. C) *ftmE* disruption: total DNA was digested with a) NheI+XbaI, or b) KpnI. WT shows a) 5.3, and b) 3.5 and 3.4 kb bands, whereas the mutant shows a) 4.2 and 3.3, and b) 9.1 kb bands. D) *ftmF* disruption: total DNA was digested with a) NdeI, or b) NruI. WT shows a) 12.9, and b) 5.2 and 3.7 kb bands, whereas the mutant shows a) 10.3 and 5.5, and b) 11.8 kb bands. E) *ftmG* disruption: total DNA was digested with a) SacII, or b) SmaI. WT shows a) 11.1, and b) 4.3 and 1.9 kb bands, whereas the mutant shows a) 7.3 and 5.5, and b) 8.2 kb bands.

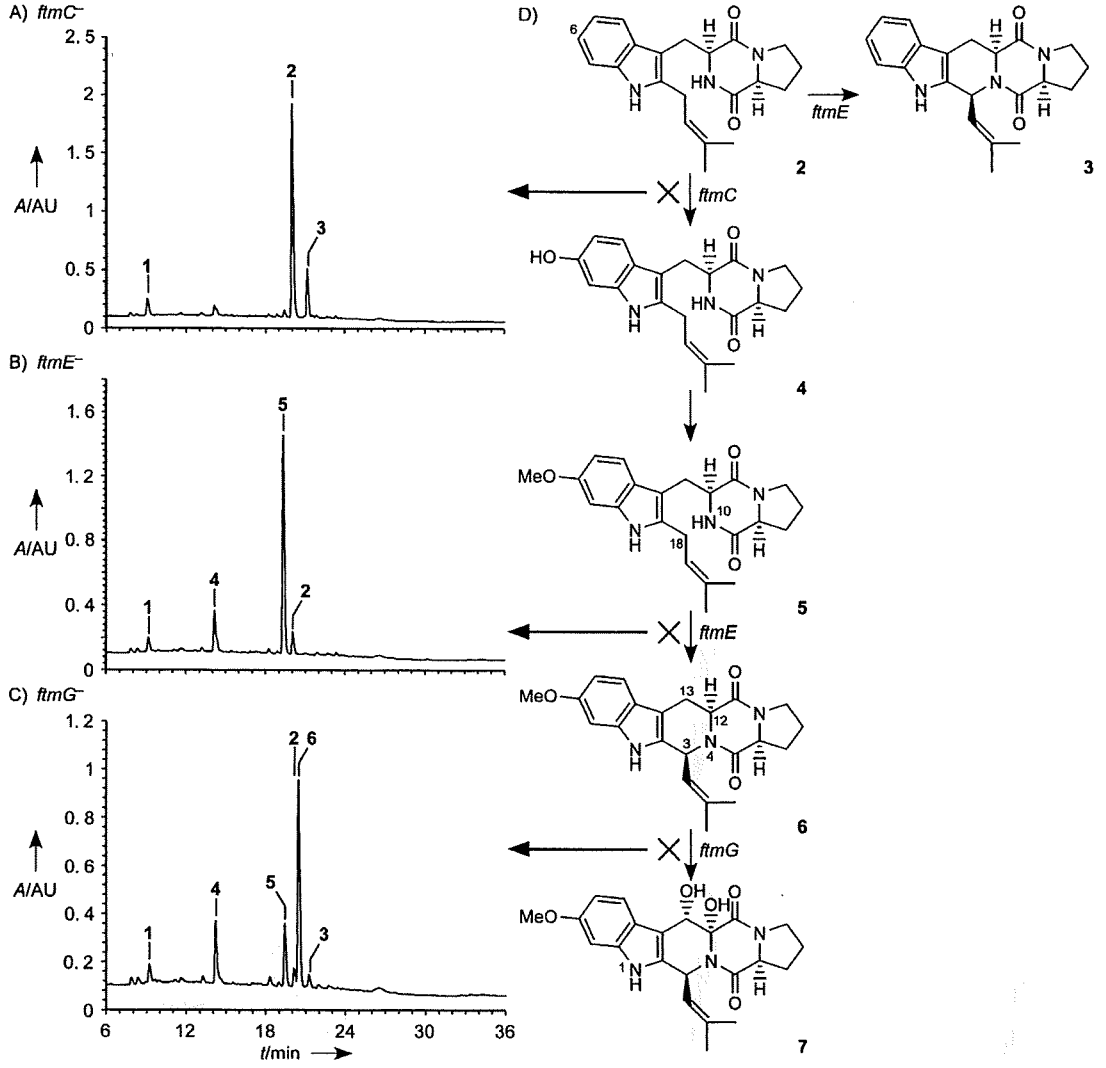

Figure 4. The metabolite profiles of the *ftm* disruptants derived from *A. fumigatus* BM939. HPLC chromatograms of culture extracts of the knockout mutants of A) *ftmC*, B) *ftmE*, and C) *ftmG*. The fungal strains were cultivated at 28 °C for 48 h. Fumitremorgins **1–8** in the culture extracts were determined by HPLC and LC/ESI-MS with reference to authentic standards. The production was analyzed independently in two to four clones of each strain. UV detection was carried out at 220 nm. D) Proposed biosynthetic pathway of fumitremorgins **3–7**.

yield **4** in the presence of NADPH (Figure 5A), even though its expression level was not high enough for the CO spectrum to be detectable. The functions of FtmE and FtmG were evaluated by bioconversion experiments: *ftmE*-expressing yeast cells converted **5** into **6** effectively (13 nM h^{-1}), whereas they also converted **2** into the shunt product **3** (6.5 nM h^{-1}; Figure 5B). Presumably these cyclizations proceeded through hydroxylation at C-18 or N-10 by FtmE, followed by dehydration to form the C–N bond. To the best of our knowledge, this is the first fungal cytochrome P450 that catalyzes C–N bond formation. Other than this, there is only one bacterial cytochrome P450, StaN, that catalyzes C–N bond formation between aglycon and deoxysugar moieties during staurosporine biosynthesis in *Streptomyces* sp. TP-A0274.[25] The conversion of **6** into **7** by *ftmG*-expressing yeast was observed, though the conversion rate was very low (4.6 nM day^{-1}; Figure 5C).

Proposed biosynthetic pathway for fumitremorgins

Previous studies have already pointed out that three genes in the *ftm* cluster—*ftmA*, *ftmB*, and *ftmH*—are involved in the first, second, and last steps, respectively, in the biosynthetic pathway of **8**.[15–17] The first committed step of the fumitremorgin pathway is the formation of **1**—diketopiperazine formation from two amino acids, L-tryptophan and L-proline. This was further supported by the lack of production of **1–8** that was observed in the *ftmA* disruptants derived from BM939 (Figure 1B). Heterologous expression of *ftmA* conferred the ability to produce **1** both to *S. cerevisiae* (data not shown) and to *A. nidulans*,[17] so **1** was obviously the biosynthetic product attributable to *ftmA* and was the precursor of **2–8**. The subsequent step is the prenylation of **1** to form **2** by FtmB/FtmPT1.[16] The other prenyltransferase, FtmH/FtmPT2, catalyzes the prenylation of the indole ring at N-1 of **7** to yield **8**.[15]

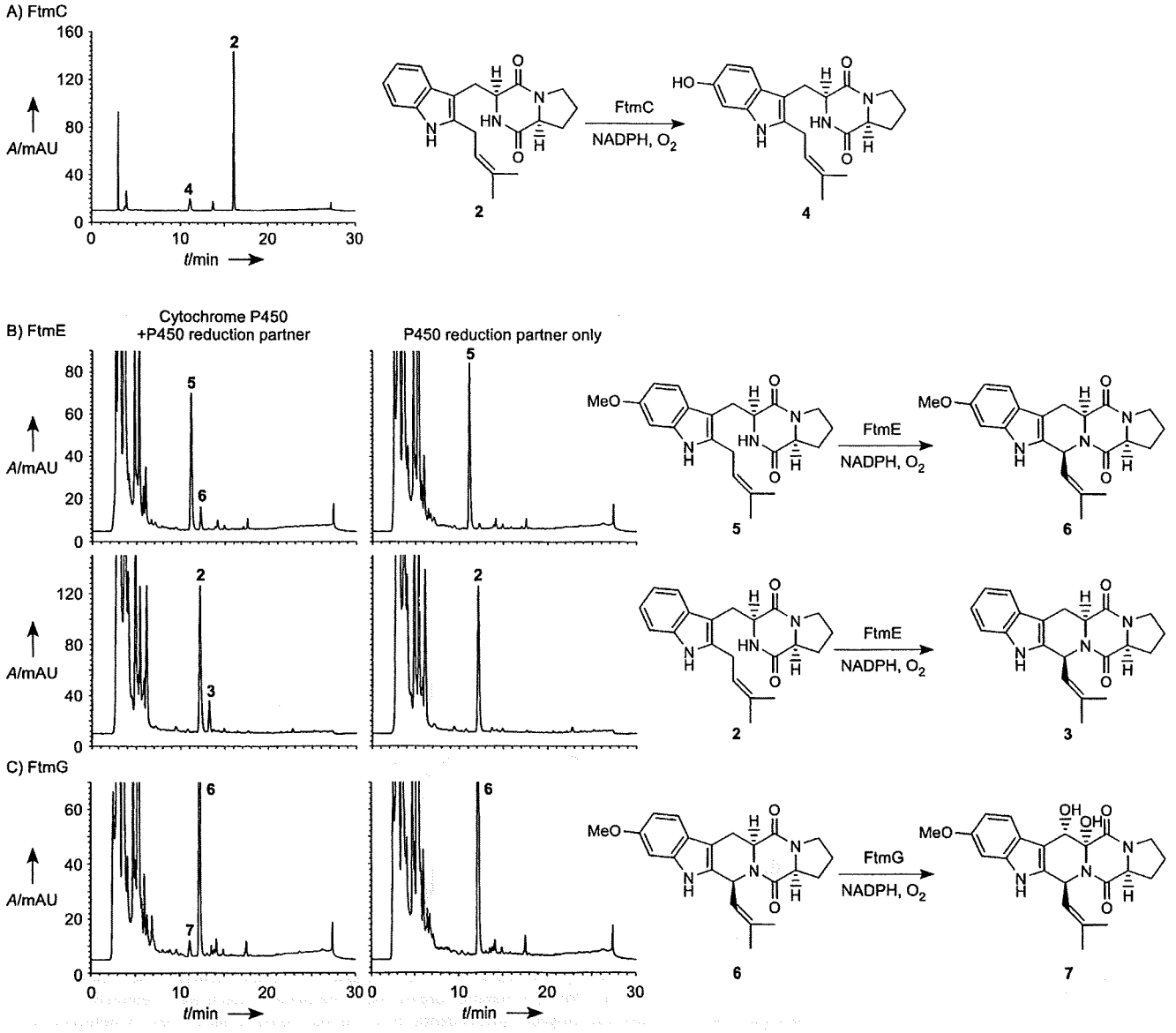

Figure 5. Reconstitution of the cytochrome P450-mediated reactions with a yeast expression system. A) HPLC chromatogram of reaction products of FtmC. Microsomes that were prepared from the yeast cells expressing *ftmC* and *AFUA_2g07940* were incubated with **2** (50 μM) in the presence of NADPH (1 mM) at 30 °C for 60 min. UV detection was carried out at 300 nm. B) HPLC chromatograms of culture extracts of the yeast cells expressing *ftmE* and *AFUA_2g07940*. The cells were incubated with substrates **5** (upper panels) and **2** (lower panels; each 2.5 μM) at 30 °C for two days. UV detection was carried out at 280 and 300 nm for reaction products of **2** and **5**, respectively. C) HPLC chromatograms of culture extracts of yeast cells expressing *ftmG* and *AFUA_2g07940*. The cells were incubated with substrate **6** (2.5 μM) at 30 °C for two days. UV detection was carried out at 300 nm.

Our results elucidated the missing link in the fumitremorgin pathway, which is composed of four processes (Figure 4D): the hydroxylation of the indole ring of **2** at C-6 by FtmC, followed by methylation to form **5**, the C–N bond formation for the synthesis of **6** by FtmE, and the subsequent hydroxylation of **6** at C-12 and C-13 by FtmG. There are three genes—*ftmD*, *ftmF*, and *ftmI*—in the cluster that remain to be characterized. Because the predicted function of FtmD is that of a methyltransferase, FtmD is a plausible candidate for the enzyme that catalyzes the methylation of **4** to form **5**.

There are several fumitremorgin-related compounds that could not be accounted for by the *ftm* gene functions. One such compound is verruculogen, which contains a unique epidioxy (C-O-O-C) bridge in its structure.[6] To date, there is no report of enzymes that catalyze epidioxy formation except for prostaglandin endoperoxide H synthase.[26] Because the functions of three out of four oxygenase genes in the cluster—*ftmC*, *ftmE* and *ftmG*—were determined, the last uncharacterized oxygenase gene, *ftmF*, might be a candidate for this interesting reaction. FtmF-dependent peroxidation is now under investigation. The disruption of *ftmI* had no significant effect on the production of **1**–**8** (data not shown), indicating that *ftmI* was unlikely to be involved in the biosynthesis of **1**–**8**.

Conclusions

Our SAR study on metabolites associated with the *ftm* cluster demonstrated that fumitremorgin C (**6**) was the most potent inhibitor against BCRP of all of the metabolites that were tested. A crucial moiety for exertion of the inhibitory activity of **6** was the covalent bond between C-3 and N-4. Methoxylation of the indole ring at C-6 and the dihydroxylation at C-12 and C-13 also modulated inhibitory activity. Targeted gene inactivation with a fumitremorgin producer strain, BM939, revealed that the three cytochrome P450 genes—*ftmC*, *ftmE*, and *ftmG*—are involved in these biosynthetic processes. We confirmed their enzymatic activities with a yeast expression system. In particular, the FtmE-mediated oxidative ring-closure step is noteworthy. To the best of our knowledge, this enzyme is the first fungal cytochrome P450 that catalyzes C–N bond formation. This study has elucidated the missing links in the fumitremorgin pathway, which are also crucial processes for exertion of the inhibitory activity of **6** against BCRP, not only providing insights into mycotoxin biosynthesis but also opening the way to improved biosynthesis of intermediates that have interesting pharmacological activities.

Experimental Section

Microbial strains and plasmids: *A. fumigatus* BM939 was isolated previously.[18] The cosmid AN26, which contains the hygromycin B-resistant cassette,[27] was obtained from the Fungal Genetics Stock Center. *E. coli* strains TOP10 and DH5α and plasmids pCR2.1-TOPO, pCR4Blunt-TOPO, pDONR P4-P1R/P2R-P3/221, and pDEST R4-R3 (Invitrogen) were used for DNA manipulation. *S. cerevisiae* YPH500 and pESC-URA (Stratagene) were used for heterologous expression of the *ftm* genes.

Preparation of fumitremorgins: *A. fumigatus* BM939 was cultivated at 28 °C for 3–5 days in complete medium [malt extract (2%), Bacto peptone (1%), glucose (2%)]. The fungal culture was cleared by filtration and extracted with ethyl acetate. From the dried extract, fumitremorgins were isolated by normal-phase chromatography on silica 60N (Kanto chemicals) followed by preparative HPLC. Their structures were determined from the following spectroscopic parameters.

Brevianamide F (1): ^{1}H NMR (500 MHz, $CDCl_3$): δ = 8.24 (brs, 1H), 7.57 (d, J = 7.8 Hz, 1H), 7.38 (d, J = 8.1 Hz, 1H), 7.21 (td, J = 7.3, 0.9 Hz, 1H), 7.12 (td, J = 7.3, 0.9 Hz, 1H), 7.09 (d, J = 1.8 Hz, 1H), 5.73 (brs, 1H), 4.36 (dd, J = 11.0, 2.8 Hz, 1H), 4.05 (t, J = 7.3 Hz, 1H), 3.74 (ddd, J = 15.1, 3.7, 0.9 Hz, 1H), 3.60 (m, 2H), 2.95 (dd, J = 15.1, 11.0 Hz, 1H), 2.30 (m, 1H), 1.99 (m, 2H), 1.89 ppm (m, 1H); ESI-MS: m/z: 284.1 $[M+H]^+$. The NMR spectra were identical to the reported data.[16]

Tryprostatin B (2): ^{1}H NMR (500 MHz, $CDCl_3$): δ = 7.94 (brs, 1H), 7.46 (d, J = 7.8 Hz, 1H), 7.29 (d, J = 8.3 Hz, 1H), 7.14 (ddd, J = 7.6, 7.1, 1.3 Hz, 1H), 7.08 (ddd, J = 10.6, 7.8, 1.0 Hz, 1H), 5.59 (brs, 1H), 5.30 (t, J = 7.0 Hz, 1H), 4.35 (brdd, J = 11.5, 2.8 Hz, 1H), 4.04 (t, J = 7.8 Hz, 1H), 3.64 (m, 2H), 3.57 (ddd, J = 11.8, 9.4, 3.2 Hz, 1H), 3.49 (dd, J = 17.6, 7.8 Hz, 1H), 3.44 (dd, J = 16.5, 6.9 Hz, 1H), 2.93 (dd, J = 15.1, 11.5 Hz, 1H), 2.31 (m, 1H), 2.05–2.00 (m, 2H), 1.95–1.85 (m, 1H), 1.77 (s, 3H), 1.74 ppm (s, 3H); ESI-MS: m/z: 352.1 $[M+H]^+$. The NMR spectra were identical to the reported data.[28]

Demethoxyfumitremorgin C (3): ^{1}H NMR (500 MHz, $CDCl_3$): δ = 7.79 (brs, 1H), 7.56 (d, J = 7.3 Hz, 1H), 7.33 (d, J = 8.1 Hz, 1H), 7.17 (brt, J = 6.3 Hz, 1H), 7.13 (brt, J = 6.9 Hz, 1H), 6.01 (d, J = 9.6 Hz, 1H), 4.90 (brd, J = 9.1 Hz, 1H), 4.17 (dd, J = 11.7, 5.0 Hz, 1H), 4.10 (brt, J = 8.2 Hz, 1H), 3.63 (m, 2H), 3.55 (dd, J = 16.0, 5.0 Hz, 1H), 3.11 (dd, J = 15.8, 11.5 Hz, 1H), 2.40 (m, 1H), 2.23 (m, 1H), 2.05 (m, 1H), 2.00 (s, 3H), 1.94 (m, 1H), 1.63 ppm (s, 3H); ESI-MS: m/z: 350.3 $[M+H]^+$. The NMR spectra were identical to the reported data.[28]

Desmethyltryprostatin A (4): Pale yellow powder; $[\alpha]_D^{21} = -25.5$ (c 0.25, in methanol); ^{1}H NMR (500 MHz, [D$_6$]DMSO): δ = 10.30 (s, 1H), 8.73 (s, 1H), 7.19 (d, J = 8.6 Hz, 1H), 7.03 (s, 1H), 6.62 (d, J = 2.3 Hz, 1H), 6.42 (dd, J = 2.3, 8.6 Hz, 1H), 5.27 (t, J = 7.0 Hz, 1H), 4.19 (t, J = 5.1 Hz, 1H), 3.98 (brdd, J = 7.3, 9.3 Hz, 1H), 3.45 (dd, J = 7.0, 15.5 Hz, 1H), 3.39 (m, 1H), 3.28 (dd, J = 7.0, 15.5 Hz, 1H), 3.17 (d, J = 4.5 Hz, 1H), 3.14 (dd, J = 5.1, 14.5 Hz, 1H), 2.90 (dd, J = 6.5, 14.5 Hz, 1H), 1.89 (m, 1H), 1.69 (s, 3H), 1.68 (s, 3H), 1.61 (m, 1H), 1.42 (m, 1H), 1.15 ppm (m, 1H); ^{13}C NMR (125 MHz, [D$_6$]DMSO): δ = 168.3 (s), 165.4 (s), 152.4 (s), 136.4 (s), 134.7 (s), 131.7 (s), 121.9 (d), 121.3 (s), 118.4 (d), 108.4 (d), 103.8 (s), 96.1 (d), 58.4 (d), 55.2 (d), 44.5 (t), 27.5 (t), 26.2 (t), 25.5 (q), 24.8 (t), 21.6 (t), 17.7 ppm (q); UV/Vis: λ_{max} = 222, 273, 299 nm; HR-FAB-MS: m/z: calcd for $C_{21}H_{26}N_3O_3$: 368.1974 $[M+H]^+$; found: 368.1980; ESI-MS: m/z: 368.3 $[M+H]^+$.

Tryprostatin A (5): ^{1}H NMR (500 MHz, $CDCl_3$): δ = 7.79 (brs, 1H), 7.32 (d, J = 8.7 Hz, 1H), 6.81 (d, J = 2.3 Hz, 1H), 6.74 (dd, J = 8.7, 2.3 Hz, 1H), 5.61 (brs, 1H), 5.28 (t, J = 7.3 Hz, 1H), 4.31 (brdd, J = 11.2, 2.7 Hz, 1H), 4.04 (t, J = 7.8 Hz, 1H), 3.81 (s, 3H), 3.63 (ddd, J = 10.2, 8.0, 3.7 Hz, 1H), 3.62 (dd, J = 15.1, 4.1 Hz, 1H), 3.57 (ddd, J = 11.9, 8.9, 2.8 Hz, 1H), 3.43 (dd, J = 17.4, 6.8 Hz, 1H), 3.39 (dd, J = 16.5, 7.3 Hz, 1H), 2.89 (dd, J = 15.1 11.5 Hz, 1H), 2.31 (m, 1H), 2.05–1.98 (m, 2H), 1.89 (m, 1H), 1.76 (d, J = 1.0 Hz, 3H), 1.73 ppm (s, 3H); ESI-MS: m/z: 382.3 $[M+H]^+$. The NMR spectra were identical to the reported data.[28]

Fumitremorgin C (6): ^{1}H NMR (500 MHz, $CDCl_3$): δ = 7.65 (brs, 1H), 7.42 (d, J = 8.3 Hz, 1H), 6.84 (d, J = 2.3 Hz, 1H), 6.79 (dd, J = 8.7, 2.3 Hz, 1H), 5.96 (d, J = 9.6 Hz, 1H), 4.89 (dt, J = 9.6, 1.4 Hz, 1H), 4.17 (dd, J = 11.9, 4.6 Hz, 1H), 4.09 (t, J = 7.8 Hz, 1H), 3.82 (s, 3H), 3.62 (m, 2H), 3.50 (dd, J = 16.0, 5.0 Hz, 1H), 3.08 (ddd, J = 15.8, 11.5, 0.9 Hz, 1H), 2.38 (m, 1H), 2.22 (m, 1H), 2.02 (m, 1H), 1.98 (d, J = 0.7 Hz, 3H), 1.94 (m, 1H), 1.63 ppm (d, J = 1.4 Hz, 3H); ESI-MS: m/z: 380.2 $[M+H]^+$. The NMR spectra were identical to the reported data.[28]

12α,13α-Dihydroxyfumitremorgin C (7): ^{1}H NMR (500 MHz, $CDCl_3$): δ = 7.78 (d, J = 8.7 Hz, 1H), 7.64 (brs, 1H), 6.83 (d, J = 2.3 Hz, 1H), 6.78 (dd, J = 8.7, 2.3 Hz, 1H), 5.85 (dd, J = 9.4, 0.9 Hz, 1H), 5.73 (dd, J = 2.8, 0.9 Hz, 1H), 4.78 (dt, J = 9.6, 1.4 Hz, 1H), 4.64 (d, J = 2.8 Hz, 1H), 4.41 (dd, J = 10.1, 6.9 Hz, 1H), 4.09 (brs, 1H), 3.82 (s, 3H), 3.62 (m, 2H), 2.47 (m, 1H), 2.08 (m, 1H), 2.02 (m, 1H), 1.99 (d, J = 1.4 Hz, 3H), 1.95 (m, 1H), 1.65 (d, J = 0.9 Hz, 3H); ESI-MS: m/z: 394.2 $[M+H-H_2O]^+$. The NMR spectra were identical to the reported data.[29]

Fumitremorgin B (8): ^{1}H NMR (500 MHz, $CDCl_3$): δ = 7.83 (d, J = 8.7 Hz, 1H), 6.78 (dd, J = 8.7, 2.3 Hz, 1H), 6.67 (d, J = 1.8 Hz, 1H), 5.97 (d, J = 10.1 Hz, 1H), 5.75 (s, 1H), 5.02 (brt, J = 6.9 Hz, 1H), 4.68 (brd, J = 10.1 Hz, 1H), 4.52 (brs, 2H), 4.43 (dd, J = 9.9, 7.3 Hz, 1H), 3.82 (s, 3H), 3.62 (dd, J = 8.9, 4.6 Hz, 2H), 2.46 (m, 1H), 2.20–1.90 (m, 3H), 1.97 (d, J = 1.4 Hz, 3H), 1.83 (s, 3H), 1.68 (d, J = 1.0 Hz, 3H), 1.61 (d, J = 1.4 Hz, 3H); ESI-MS: m/z: 462.1 $[M+H-H_2O]^+$. The NMR spectra were identical to the reported data.[30]

BCRP inhibitory assay: The BCRP inhibitory activities of fumitremorgins **1**–**8** were assessed by growth inhibition of K562 cells that

overexpressed the BCRP gene (K562/BCRP) by the anticancer drug SN-38, as described previously.[31] Briefly, K562/BCRP cells were grown in RPMI 1640 medium that was supplemented with fetal bovine serum (7%, *v/v*) at 37 °C in CO_2 (5%, *v/v*). The sensitivity of the K562/BCRP cells to SN-38 in the presence of fumitremorgins (3 μM) was evaluated by cell growth inhibition after incubation at 37 °C for 4 days. Cell numbers were determined with a Coulter counter. The IC_{50} values (drug dose that caused 50% inhibition of cell growth) were determined from the growth inhibition curves.

The inhibitory effects of fumitremorgins **1**–**8** on BCRP activity were also evaluated in vitro by measuring BCRP-dependent ATPase activity, as described previously,[32] with minor modifications. BCRP membranes (BD Biosciences) were incubated at 37 °C in medium (95 μL) consisting of Tris-MES (50 mM, pH 6.8), EGTA (2 mM), DTT (2 mM), KCl (50 mM), sodium azide (5 mM), and fumitremorgins (50 μM). The ATPase reaction was started by the addition of MgATP (100 mM, 5 μL). To measure BCRP-independent ATPase activity, an identical reaction mixture that contained sodium orthovanadate (400 μM) was assayed in parallel. After incubation for 30 min, reactions were terminated by addition of perchloric acid (0.6 M, 100 μL). The amount of inorganic phosphate was determined as described previously.[33]

Cloning of the *ftm* cluster of *A. fumigatus* BM939: An AflII site was introduced into the cloning site of a cosmid vector (SuperCos1, Stratagene). The resulting vector was used for construction of a genomic library of *A. fumigatus* BM939 with AflII-digested chromosomal DNA of the strain. On screening of the library, a 27 kb cosmid clone that covered the *ftm* genes was isolated.

Disruption of the *ftm* genes: We first prepared the *akuA*-disrupted strain derived from *A. fumigatus* BM939. The *akuA* gene encodes the Ku70 component that causes low efficiency of homologous recombination in filamentous fungi.[34,35] For construction of the *akuA* knockout plasmids, 1 kb DNA fragments upstream of the start codon and downstream of the stop codon of *akuA* were amplified by PCR with use of chromosomal DNA of *A. fumigatus* BM939 as template. The primer pairs *akuA*-UF(−1023)/*akuA*-UR(−16) and *akuA*-DF(2269)/*akuA*-DR(3265) were used for amplification of the upstream and downstream regions, respectively. The pyrithiamine-resistant gene *ptrA*[36] was used as a selection marker for the *akuA* knockout. These DNA fragments were combined in the original orientation in pDEST by use of the MultiSite Gateway System (Invitrogen) in the following order: the upstream region, *ptrA*, followed by the downstream region. From this plasmid, a DNA fragment (4.0 kb) was excised by KpnI digestion and used for transformation of *A. fumigatus* BM939. Pyrithiamine-resistant transformants (Δ*akuA*::*ptrA*) that resulted from double-crossover between the disrupted *akuA* sequence and the intact chromosomal *akuA* sequence were isolated. Correct disruption was checked by Southern hybridization (data not shown). The resulting *akuA*$^-$ strain TAFK1.39 was used as a recipient strain for further transformations.

Knockout mutants of the *ftm* genes were prepared from TAFK1.39, in a procedure similar to that described for the *akuA* disruption. The 1 kb DNA fragments upstream and downstream of the *ftm* genes were amplified by PCR with use of chromosomal DNA of BM939 as template. The primer pairs *ftm*-UF and -UR and *ftm*-DF and -DR were used for amplification of the upstream and downstream regions, respectively. The hygromycin B-resistant cassette (*hph*) was used as a selection marker. These DNA fragments were combined in the original orientation in pDEST in the following order: the upstream regions, *hph*, followed by the downstream regions. From these plasmids, 5.9 kb DNA fragments were excised by restriction enzyme digestion and used for fungal transformation. The restriction enzymes that were used are indicated in Table S2. Hygromycin B-resistant transformants (Δ*ftm*::*hph*) were verified by genomic Southern analysis to contain the *ftm* gene replacements (Figure 3). Note that the parent *akuA* strain TAFK1.39 is described as the "wild-type" strain in this study. All of the DNA fragments amplified by PCR were verified by sequencing. The oligonucleotides that were used for PCR are summarized in Table S2.

Determination of fumitremorgins produced by the *ftm* disruptants: Freshly harvested spore suspensions of an *A. fumigatus* strain were inoculated in fermentation medium [K_2HPO_4 (0.5%), $MgSO_4{\cdot}7H_2O$ (0.05%), soybean meal (2%), glucose (3%), soluble starch (2%), pH 6.5]. The culture was cultivated at 28 °C for 48 h and cleared by filtration. The culture filtrate was extracted with ethyl acetate. The dried extracts were dissolved in methanol and analyzed by HPLC and LC/ESI-MS.

HPLC analysis was carried out with a Waters 600 HPLC system with a photodiode array detector (2996 PDA detector). The HPLC conditions were as follows: column, Senshu Pak Docosil-B 3 μ (4.6× 250 mm); flow rate, 1.0 mL min^{-1}; solvent A, water containing formic acid (0.05%, *v/v*); solvent B, acetonitrile. After injection of the sample into a column equilibrated with solvent B (25%), the column was developed with a linear gradient from 25% to 65% over 20 min, followed by isocratic elution of solvent B (65%) for 20 min. LC/ESI-MS analysis was carried out with a Waters Alliance HPLC system fitted with a mass spectrometer (Q-TRAP, Applied Biosystems). The HPLC conditions were as follows: column, Senshu Pak Docosil-B 3 μ (2.0×250 mm, Senshu Scientific); flow rate, 0.2 mL min^{-1}. After injection of the sample into a column equilibrated with solvent B (10%), the column was developed with a linear gradient from 10% to 100% solvent B over 90 min. Mass spectra were collected in an ESI-positive mode.

Construction of plasmids for heterologous expression of the *ftm* genes: The ORFs of *AFUA_2g07940* and *ftmE* were amplified by PCR with chromosomal DNA of *A. fumigatus* BM939 as template. The ORFs of *ftmC* and *ftmG* were amplified by two-step RT-PCR with total RNA extracted from *A. fumigatus* BM939 as template. All DNA fragments amplified by PCR were cloned into pCR4Blunt-TOPO and verified by sequencing. The *AFUA_2g07940* ORF in pCR4Blunt-TOPO was excised by SalI–XhoI digestion and cloned into the SalI-XhoI site of pESC-URA, resulting in pEUR07940. The ORFs of *ftmC*, *ftmE*, and *ftmG* were cloned in the NotI–SpeI site of pEUR079490, resulting in pEUR07940-*ftmC*, -*ftmE*, and -*ftmG*, respectively. These plasmids contained *AFUA_2g07940* and the *ftm* gene under the *GAL1* and *GAL10* promoters, respectively. The oligonucleotides that were used for PCR are summarized in Table S3.

In vitro assay of FtmC: *S. cerevisiae* YPH500 containing pEUR07940-*ftmC* was cultivated at 30 °C for three days in SGI medium [yeast nitrogen base (0.7%), galactose (2%), casamino acids (0.1%), with L-tryptophan and L-histidine (20 mg L^{-1}), L-leucine (30 mg L^{-1}), and adenine (200 mg L^{-1})]. From the harvested cells, microsomes were prepared as described previously.[37] The CO spectrum was undetectable. The reaction mixture (500 μL) consisted of Tris·HCl (50 mM, pH 7.5), glycerol (20%, *v/v*), 2-mercaptoethanol (15 mM), fumitremorgin substrate (50 μM), NADPH (1 mM), and microsomes. After the reaction mixtures had been incubated at 30 °C for 60 min, the reactions were terminated by addition of HCl (a final concentration of 0.1 M). Reaction products were extracted with ethyl acetate and analyzed by HPLC and LC/ESI-MS.

Bioconversion assay of FtmE and FtmG: *S. cerevisiae* YPH500 carrying pEUR07940-*ftmE* or -*ftmG* was cultivated at 30 °C for 1 day in SGI medium. After fumitremorgin substrates had been added to the cultures (final concentrations of 2.5 μM), the cultures were further incubated for two days. The compounds in the broths were extracted with ethyl acetate and analyzed by HPLC and LC/ESI-MS.

The following conditions were used for HPLC analysis of the reaction products of in vitro and bioconversion assays: column, Senshu Pak Docosil-B (4.6×250 mm); flow rate, 1.0 mL min $^{-1}$. After injection of the sample into a column equilibrated with 20% solvent B, the column was initially developed isocratically for 3 min. The column was successively developed with a linear gradient 20% to 100% over 15 min, isocratic elution for 1 min, a linear gradient 100% to 20% over 1 min, followed by isocratic elution of solvent B (20%) over 10 min.

Accession numbers: The nucleotide sequence reported in this paper has been deposited to the GenBank/DDBJ/EMBL database under accession number AB436628.

Acknowledgements

We are grateful to Y. Koyama (Noda Institute for Scientific Research) for valuable discussions. We also thank S. Simizu, H. Ichimiya, and S. Kazami for evaluation of the bioactivities of the compounds, and T. Saito for advice and support. This work was supported in part by a Grant-in-Aid for Creative Scientific Research from the Ministry of Education, Culture, Sports, Science, and Technology of Japan, and by funding from the Special Postdoctoral Researchers Program of RIKEN (to N.K. and H.S.).

Keywords: *Aspergillus fumigatus* · biosynthesis · cytochrome P450 · fumitremorgins · natural products

[1] L. A. Doyle, D. D. Ross, *Oncogene* **2003**, *22*, 7340–7358.
[2] P. Krishnamurthy, J. D. Schuetz, *Annu. Rev. Pharmacol. Toxicol.* **2006**, *46*, 381–410.
[3] S. Zhou, J. D. Schuetz, K. D. Bunting, A. M. Colapietro, J. Sampath, J. J. Morris, I. Lagutina, G. C. Grosveld, M. Osawa, H. Nakauchi, B. P. Sorrentino, *Nat. Med.* **2001**, *7*, 1028–1034.
[4] M. de Bruin, K. Miyake, T. Litman, R. Robey, S. E. Bates, *Cancer Lett.* **1999**, *146*, 117–126.
[5] F. Hyafil, C. Vergely, P. Du Vignaud, T. Grand-Perret, *Cancer Res.* **1993**, *53*, 4595–4602.
[6] R. J. Cole, M. A. Schweikert in *Handbook of Secondary Fungal Metabolites, Vol. 1* (Eds.: R. J. Cole, M. A. Schweikert, B. B. Jarvis), Academic Press, San Diego, **2003**, pp. 222–232.
[7] S. K. Rabindran, H. He, M. Singh, E. Brown, K. I. Collins, T. Annable, L. M. Greenberger, *Cancer Res.* **1998**, *58*, 5850–5858.
[8] S. K. Rabindran, D. D. Ross, L. A. Doyle, W. Yang, L. M. Greenberger, *Cancer Res.* **2000**, *60*, 47–50.
[9] J. D. Allen, A. van Loevezijn, J. M. Lakhai, M. van der Valk, O. van Tellingen, G. Reid, J. H. Schellens, G. J. Koomen, A. H. Schinkel, *Mol. Cancer Ther.* **2002**, *1*, 417–425.
[10] A. van Loevezijn, J. D. Allen, A. H. Schinkel, G. J. Koomen, *Bioorg. Med. Chem. Lett.* **2001**, *11*, 29–32.
[11] W. C. Nierman, A. Pain, M. J. Anderson, J. R. Wortman, H. S. Kim, J. Arroyo, M. Berriman, K. Abe, D. B. Archer, C. Bermejo, J. Bennett, P. Bowyer, D. Chen, M. Collins, R. Coulsen, R. Davies, P. S. Dyer, M. Farman, N. Fedorova, N. Fedorova, T. V. Feldblyum, R. Fischer, N. Fosker, A. Fraser, J. L. Garcia, M. J. Garcia, A. Goble, G. H. Goldman, K. Gomi, S. Griffith-Jones, R. Gwilliam, B. Haas, H. Haas, D. Harris, H. Horiuchi, J. Huang, S. Humphray, J. Jimenez, N. Keller, H. Khouri, K. Kitamoto, T. Kobayashi, S. Konzack, R. Kulkarni, T. Kumagai, A. Lafon, J. P. Latge, W. Li, A. Lord, C. Lu, W. H. Majoros, G. S. May, B. L. Miller, Y. Mohamoud, M. Molina, M. Monod, I. Mouyna, S. Mulligan, L. Murphy, S. O'Neil, I. Paulsen, M. A. Penalva, M. Pertea, C. Price, B. L. Pritchard, M. A. Quail, E. Rabbinowitsch, N. Rawlins, M. A. Rajandream, U. Reichard, H. Renauld, G. D. Robson, S. Rodriguez de Cordoba, J. M. Rodriguez-Pena, C. M. Ronning, S. Rutter, S. L. Salzberg, M. Sanchez, J. C. Sanchez-Ferrero, D. Saunders, K. Seeger, R. Squares, S. Squares, M. Takeuchi, F. Tekaia, G. Turner, C. R. Vazquez de Aldana, J. Weidman, O. White, J. Woodward, J. H. Yu, C. Fraser, J. E. Galagan, K. Asai, M. Machida, N. Hall, B. Barrell, D. W. Denning, *Nature* **2005**, *438*, 1151–1156.
[12] D. M. Gardiner, B. J. Howlett, *FEMS Microbiol. Lett.* **2005**, *248*, 241–248.
[13] S. Maiya, A. Grundmann, X. Li, S. M. Li, G. Turner, *ChemBioChem* **2007**, *8*, 1736–1743.
[14] I. A. Unsold, S. M. Li, *Microbiology* **2005**, *151*, 1499–1505.
[15] A. Grundmann, T. Kuznetsova, S. S. Afiyatullov, S. M. Li, *ChemBioChem* **2008**, *9*, 2059–2063.
[16] A. Grundmann, S. M. Li, *Microbiology* **2005**, *151*, 2199–2207.
[17] S. Maiya, A. Grundmann, S. M. Li, G. Turner, *ChemBioChem* **2006**, *7*, 1062–1069.
[18] C. B. Cui, H. Kakeya, G. Okada, R. Onose, H. Osada, *J. Antibiot.* **1996**, *49*, 527–533.
[19] H. Woehlecke, H. Osada, A. Herrmann, H. Lage, *Int. J. Cancer* **2003**, *107*, 721–728.
[20] L. Wang, K. Sasai, T. Akagi, S. Tanaka, *Biochem. Biophys. Res. Commun.* **2008**, *373*, 392–396.
[21] T. Usui, M. Kondoh, C. B. Cui, T. Mayumi, H. Osada, *Biochem. J.* **1998**, *333*, 543–548.
[22] H. D. Jain, C. Zhang, S. Zhou, H. Zhou, J. Ma, X. Liu, X. Liao, A. M. Deveau, C. M. Dieckhaus, M. A. Johnson, K. S. Smith, T. L. Macdonald, H. Kakeya, H. Osada, J. M. Cook, *Bioorg. Med. Chem.* **2008**, *16*, 4626–4651.
[23] E. De Carolis, V. De Luca, *Phytochemistry* **1994**, *36*, 1093–1107.
[24] S. G. Sedgwick, S. J. Smerdon, *Trends Biochem. Sci.* **1999**, *24*, 311–316.
[25] H. Onaka, S. Asamizu, Y. Igarashi, R. Yoshida, T. Furumai, *Biosci. Biotechnol. Biochem.* **2005**, *69*, 1753–1759.
[26] W. L. Smith, R. M. Garavito, D. L. DeWitt, *J. Biol. Chem.* **1996**, *271*, 33157–33160.
[27] P. J. Punt, R. P. Oliver, M. A. Dingemanse, P. H. Pouwels, C. A. van den Hondel, *Gene* **1987**, *56*, 117–124.
[28] C. B. Cui, H. Kakeya, H. Osada, *J. Antibiot.* **1996**, *49*, 534–540.
[29] W.-R. Abraham, H.-A. Arfmann, *Phytochemistry* **1990**, *29*, 1025–1026.
[30] S. Kodato, M. Nakagawa, M. Hongu, T. Kawate, T. Hino, *Tetrahedron* **1988**, *44*, 359–377.
[31] K. Katayama, K. Masuyama, S. Yoshioka, H. Hasegawa, J. Mitsuhashi, Y. Sugimoto, *Cancer Chemother. Pharmacol.* **2007**, *60*, 789–797.
[32] B. Sarkadi, E. M. Price, R. C. Boucher, U. A. Germann, G. A. Scarborough, *J. Biol. Chem.* **1992**, *267*, 4854–4858.
[33] J. Nakazawa, J. Yajima, T. Usui, M. Ueki, A. Takatsuki, M. Imoto, Y. Y. Toyoshima, H. Osada, *Chem. Biol.* **2003**, *10*, 131–137.
[34] S. Krappmann, C. Sasse, G. H. Braus, *Eukaryotic Cell* **2006**, *5*, 212–215.
[35] Y. Ninomiya, K. Suzuki, C. Ishii, H. Inoue, *Proc. Natl. Acad. Sci. USA* **2004**, *101*, 12248–12253.
[36] T. Kubodera, N. Yamashita, A. Nishimura, *Biosci. Biotechnol. Biochem.* **2000**, *64*, 1416–1421.
[37] S. Takahashi, Y. Zhao, P. E. O'Maille, B. T. Greenhagen, J. P. Noel, R. M. Coates, J. Chappell, *J. Biol. Chem.* **2005**, *280*, 3686–3696.

Received: November 28, 2008
Published online on February 18, 2009

Available online at www.sciencedirect.com
ScienceDirect
Bioorganic & Medicinal Chemistry
ELSEVIER
Bioorganic & Medicinal Chemistry 16 (2008) 4626–4651

Synthesis and structure–activity relationship studies on tryprostatin A, an inhibitor of breast cancer resistance protein

Hiteshkumar D. Jain,[a] Chunchun Zhang,[a] Shuo Zhou,[a] Hao Zhou,[a] Jun Ma,[a] Xiaoxiang Liu,[a] Xuebin Liao,[a] Amy M. Deveau,[a] Christine M. Dieckhaus,[b] Michael A. Johnson,[b] Kirsten S. Smith,[b] Timothy L. Macdonald,[b] Hideaki Kakeya,[c] Hiroyuki Osada[c] and James M. Cook[a,*]

[a]*Department of Chemistry, University of Wisconsin—Milwaukee, Milwaukee, WI 53201, USA*
[b]*Department of Chemistry, University of Virginia, McCormick Road, Charlottesville, VA 22904, USA*
[c]*Antibiotics Laboratory, Discovery Research Institute, RIKEN, 2-1 Hirosawa, Wako-shi, Saitama 351-0198, Japan*

Received 7 December 2007; revised 10 February 2008; accepted 11 February 2008
Available online 20 February 2008

Abstract—Tryprostatin A is an inhibitor of breast cancer resistance protein, consequently a series of structure–activity studies on the cell cycle inhibitory effects of tryprostatin A analogues as potential antitumor antimitotic agents have been carried out. These analogues were assayed for their growth inhibition properties and their ability to perturb the cell cycle in tsFT210 cells. SAR studies resulted in the identification of the essential structural features required for cytotoxic activity. The absolute configuration L-Tyr-L-pro in the diketopiperazine ring along with the presence of the 6-methoxy substituent on the indole moiety of **1** was shown to be essential for dual inhibition of topoisomerase II and tubulin polymerization. Biological evaluation also indicated the presence of the 2-isoprenyl moiety on the indole scaffold of **1** was essential for potent inhibition of cell proliferation. Substitution of the indole N_a–H in **1** with various alkyl or aryl groups, incorporation of various L-amino acids into the diketopiperazine ring in place of L-proline, and substitution of the 6-methoxy group in **1** with other functionality provided active analogues. The nature of the substituents present on the indole N_a–H or the indole C-2 position influenced the mechanism of action of these analogues. Analogues **68** (IC_{50} = 10 μM) and **67** (IC_{50} = 19 μM) were 7-fold and 3.5-fold more potent, respectively, than **1** (IC_{50} = 68 μM) in the inhibition of the growth of tsFT210 cells. Diastereomer-2 of tryprostatin B **8** was a potent inhibitor of the growth of three human carcinoma cell lines: H520 (IC_{50} = 11.9 μM), MCF-7 (IC_{50} = 17.0 μM) and PC-3 (IC_{50} = 11.1 μM) and was equipotent with etoposide, a clinically used anticancer agent. Isothiocyanate analogue **71** and 6-azido analogue **72** were as potent as **1** in the tsFT210 cell proliferation and may be useful tools in labeling BCRP.

1. Introduction

The cell cycle coordinates a variety of cellular functions involved in the accurate replication of the genome and cell division.[1] These processes are tightly regulated primarily at the G_1/S and G_2/M phase transitions by a series of checkpoints. It has become clear that checkpoint control defects in cancer cells contribute to tumorigenesis and are a significant reason for the increased selectivity of tumors over normal cells towards chemotherapy.[2,3] Cell cycle inhibitors or modulators are highly promising new therapeutic agents against human cancers.

With an increased understanding of the molecular biology of cell cycle control it has become possible to develop bioassays and screen for agents that specifically interfere with these processes. One such method was developed by Osada et al.[4,5] which utilizes the synchronous culture of the murine temperature-sensitive mutant cell line, tsFT210, defective in the $p34^{cdc2}$ gene. With this assay a family of 2-isoprenylated diketopiperazine indole alkaloids which effect cell cycle arrest at the G2/M phase was isolated from the fermentation broth of a marine fungal strain of *Aspergillus fumigatus* BM939. It was found that tryprostatin A **1** (Chart 1) and tryprostatin B **2** (Chart 1) completely inhibited cell cycle

Keywords: Tryprostatin A; Antimitotic; Anticancer; Breast cancer resistance protein.
* Corresponding author. Tel.: +1 414 229 5856; fax: +1 414 229 5530; e-mail: capncook@uwm.edu

0968-0896/$ - see front matter © 2008 Elsevier Ltd. All rights reserved.
doi:10.1016/j.bmc.2008.02.050

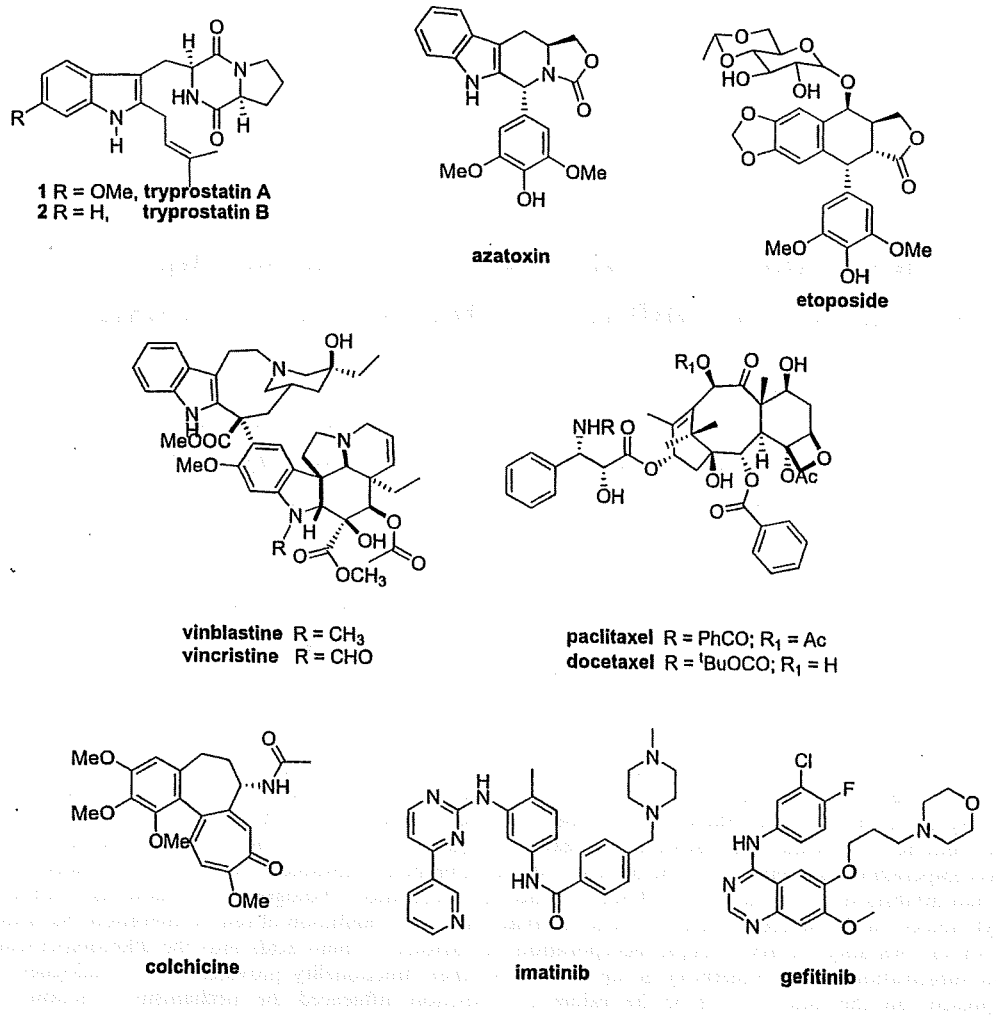

Chart 1.

progression of tsFT210 cells in the G2/M phase at a final concentration of 50 μg/mL of **1** and 12.5 μg/mL of **2**, respectively.[6–8] Since these indole alkaloids were isolated only in small amounts, studies on the mechanism and SAR were not reported earlier.

Tryprostatin A and B have previously been synthesized,[9–11] the aim of which was to study their mechanism of action. The similarities in the structures of the tryprostatins with etoposide (Chart 1) and azatoxin (Chart 1), a dual inhibitor of topoisomerase II (G2)/tubulin polymerization (M), led to the investigation of the ability of the two tryprostatins to inhibit topoisomerase II and tubulin polymerization. Biological evaluations[12] of **1** and **2** indicated that both alkaloids were very weak inhibitors of topoisomerase II in the topoisomerase II assay; while only **1** had marginal activity in the tubulin polymerization assay. This latter result was in agreement with the data reported for **1** by Osada et al.[13] Osada et al.[13] also reported **1** inhibited cell cycle progression of rat normal fibroblast 3Y1 cells specifically in the M phase. The concentration of **1** that arrested cell cycle progression in the M phase corresponded to that which induced a marked depolymerization *in situ* of the microtubules containing both cytoplasmic network and spindle apparatus. Although tryprostatin B **2** arrested cell cycle progression at a lower concentration than **1**, the inhibition was not due to inhibition of the M phase. It was shown that **1** inhibited microtubule assembly through a different type of mechanism than colchicine (Chart 1), vinblastine (Chart 1), or maytansine–rhizoxin.[13] Tryprostatin A **1** inhibited microtubule assembly by interfering with the interaction between microtubule-associated proteins (MAPs) and the C-terminal domain of tubulin. Since **1** operated by an entirely novel mechanism this may be important in cancer chemotherapy, especially in multiple drug resistance (MDR) cancers.

Microtubules are hollow cylindrical tubes found in almost all eukaryotic cell types. They play an important role in a variety of cellular functions, such as cell division, cell movement, cell shape, and transport of organelles inside the cell.[14] Tubulin exists as a heterodimer of α- and β-tubulin and is the major building block of microtubules. Proteins such as the MAPs bind to and modify microtubule properties.[14,15] In the absence of MAPs, α/β-tubulin heterodimers polymerize only by treatment with high concentrations of glycerol or organic acids such as glutamate.[16]

The discovery of numerous compounds from natural sources which display a wide structural diversity and are cytotoxic by perturbation of the dynamic instability of microtubules has attracted much attention within the last two decades.[17–20] Microtubules have, therefore, become an attractive pharmacological target for anticancer drug discovery.[17–20] Almost all antimitotic agents interact with the α/β-tubulin dimer, rather than microtubule-associated proteins (MAPs) or other proteins involved in microtubule functions. The *Vinca* alkaloids, exemplified by vinblastine (Chart 1) and vincristine (Chart 1), as well as the taxanes, such as paclitaxel (Chart 1) and the semisynthetic analogue docetaxel (Chart 1), are the most commonly used antimitotic agents in the clinical treatment of cancer.[21] Colchicine is another important antimitotic agent; however, it has limited medicinal utility due to its narrow therapeutic index.

Additionally, the natural products combretastatin A-4,[22] curacin A,[23] podophyllotoxin,[24] epothilones A and B,[25] and dolastatin[26] to cite just a few, are known to be cytotoxic through binding interactions with tubulin. Another antimitotic agent, estramustine phosphate inhibits microtubule assembly by binding to both microtubule-associated protein 2 (MAP2) and tubulin,[27] while 5,5′-bis[8-(phenylamino)-1-naphthalenesulphonate] (bis-ANS) specifically inhibits MAP-dependent microtubule assembly by interaction with the C-terminal domain of the tubulin heterodimer.[28] These compounds may lead to useful cancer therapeutic agents. Indeed, estramustine in combination with other antimicrotubule agents exhibits synergistic cytotoxicity both in vitro and in vivo.[27] However, no new tubulin polymerization inhibitor of low molecular weight has reached clinical status, as yet. Clinically available compounds such as paclitaxel or vincristine face several disadvantages; principally: (i) high toxicity, (ii) development of drug resistance in patients, (iii) marginal oral bioavailability and poor solubility, and (iv) complex synthesis or isolation procedures.[17–20] Therefore, a pressing need to develop simpler, more effective antitumor drugs still remains.

The development of MDR to chemotherapeutic agents remains one of the primary obstacles in cancer treatment. These arise from intrinsic or acquired mechanisms of resistance. The overexpression of energy dependent (ATP) transmembrane drug-efflux pumps, such as P-glycoprotein (MDR1), multidrug resistance protein (MRP), and breast cancer resistance protein (BCRP), have been shown to produce resistance to several commonly used chemotherapeutic agents. Breast cancer resistance protein is a 72 kDa protein which probably homodimerizes to form an active transport complex.[29] BCRP was first identified in drug resistant MCF-7/adrVp cells[30] and has been recently reviewed.[31–33] Like other members of the ATP binding cassette family of membrane transporters, such as MDR1 and MRP1, BCRP is expressed in a variety of malignancies where it may produce resistance to chemotherapeutic agents. In addition, it has also been reported that BCRP expression may be a prognostic indicator in certain cancers and is associated with poor response to chemotherapy.[34,35] Overexpression of BCRP has been reported in a number of tumor types including: adenocarcinomas (arising from the digestive tract, the endometrium, and the lung), melanoma, soft tissue sarcomas,[36] hematological malignancies such as acute myeloid leukemia (AML),[37] and acute lymphoblastic leukemia (ALL).[38] Elevated expression of BCRP results in resistance of various cancer cell lines to antitumor drugs including: topotecan, mitoxantrone, daunorubicin, doxorubicin, and bisantrene.[39] In addition, flavopiridol resistance is mediated by BCRP.[40]

The clinical significance of BCRP along with its limited expression in normal tissues makes BCRP a viable target for inhibition to reverse MDR. Several potent and specific inhibitors of BCRP have been developed. This has potentially opened the door to clinical applications of BCRP inhibition. These inhibitors include the

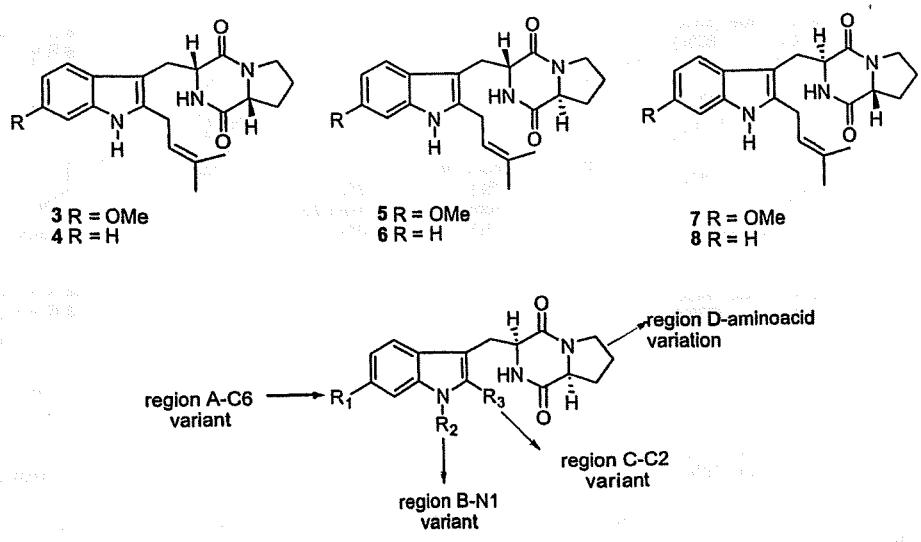

Figure 1.

targeted agents: gefitinib and imatinib mesylate,[41] as well as the more specific inhibitors: fumitremorgin C,[42] tryprostatin A,[43] and GF120918.[44] At concentrations of 10–50 μM, tryprostatin A **1** was shown to reverse a mitoxantrone-resistant phenotype and inhibited the cellular BCRP-dependent mitoxantrone accumulation in the human gastric carcinoma cell line EPG85-257RNOV and the human breast cancer cell line MCF-7/AdrVp (both exhibited acquired BCRP-mediated MDR). No cytotoxicity was observed at effective concentrations.[43]

In the search for potent and selective antitumor agents, the synthesis of a series of analogues (**3–8**, Fig. 1) of **1** and **2** was carried out in order to probe the importance of the stereochemistry of the diketopiperazine ring on the inhibition of topoisomerase II and/or tubulin polymerization. Tryprostatin analogues **1–8** were evaluated for their ability to inhibit topoisomerase II and/or tubulin binding protein as well as their tumor cell growth inhibitory activity.[12]

More recently, Osada et al.[13] reported the presence of the 6-methoxy substituent on the indole moiety of **1** conferred lower cytotoxicity to tryprostatin A and enhanced the specificity for inhibition of microtubule assembly. The lower cytotoxicity of **1** in comparison to **2**, combined with a unique mechanism for inhibition of tubulin polymerization, as well as BCRP prompted investigation of the structure activity relationships (SAR) in **1** in order to enhance tubulin polymerization and/or BCRP inhibition. To our knowledge, no SAR of tryprostatin A has appeared in the literature, to date. The SAR studies were designed to determine the minimum structural requirements of tryprostatin A required to exhibit potent and selective cytotoxic activity, in the search for new anticancer agents. Several modifications, which maintained the same backbone, were carried out as outlined in Figure 1: (A) substitution of the 6-position of the aromatic ring, (B) alkylation of the indole NH, (C) substitution of the 2-position of the indole moiety, and (D) substitution of the L-proline residue in the diketopiperazine ring with other L-amino acids.

2. Chemistry

The synthesis of optically active **1** and **2** have been reported.[9–11] This method was also extended to the synthesis of the enantiomers (**3** and **4**) and diastereomers (**5–8**) of **1** and **2** (Scheme 1).[11,12] The synthesis of **1–8**

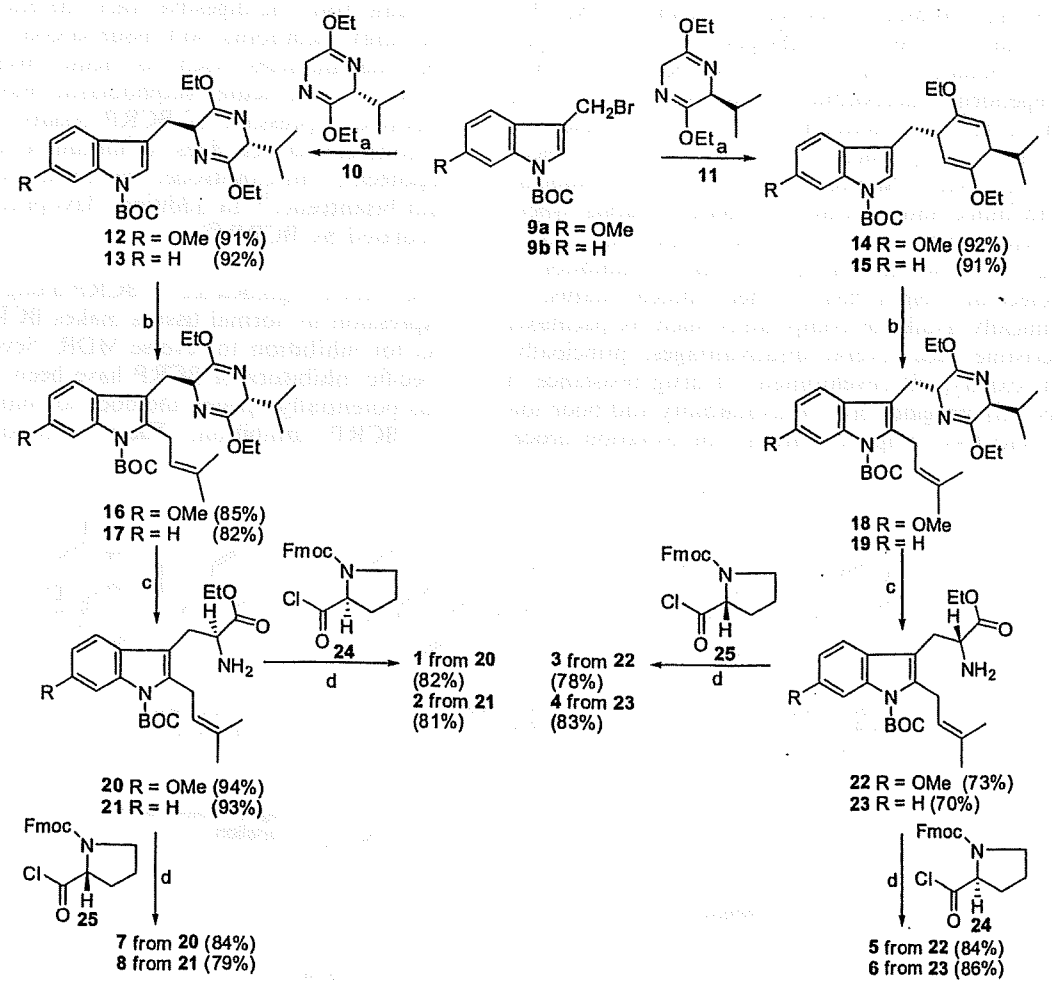

Scheme 1. Reagents and conditions: (a) THF, *n*-BuLi, −78 °C; (b) LDA (1.5 equiv), THF, isoprenylbromide (3 equiv); (c) 2 N aq HCl, THF, −78 °C to rt; (d) TEA, $CHCl_3$; DEA, CH_3CN, rt; xylene, reflux.

(Scheme 1) began with indoles **9a** and **9b** which were coupled with the anion of the Schöllkopf chiral auxiliary **11** (derived from L-valine), to afford the *trans* diastereomers **14** and **15**, respectively, with 100% diastereoselectivity. The diastereoselectivity of the addition to the Schöllkopf chiral auxillary was found to be 100% by analysis of the ^1H spectrum of the crude mixture of the respective compounds. When indoles **14** and **15** were treated with LDA at −78 °C, followed by addition of isoprenyl bromide, the 2-isoprenylpyrazine derivatives **18** and **19** were obtained, respectively. The pyrazine moiety was removed from pyrazines **18** or **19** under acidic conditions (aq HCl, THF) in 94% yield to afford the 2-isoprenyl tryptophan **22** or **23**, respectively. The coupling of 2-isoprenyl tryptophan **22** or **23** with Fmoc-D-proline **25** using triethylamine as the base was followed by formation of the diketopiperazine ring. The Boc protecting group was removed from the indole N(H) function in refluxing xylene to afford **3** and **4**, respectively. Similarly, coupling of 2-isoprenyl tryptophan **22** or **23** with Fmoc-L-proline **24** afforded **5** or **6**, respectively. The natural products (**1** and **2**) were prepared from the *trans* transfer of chirality from D-valine (Schöllkopf) and from L-proline.[9–11] The diastereomers **7** and **8** of **1** and **2**, respectively, were prepared from the *trans* transfer of chirality from D-valine (Schöllkopf) and from D-proline, as outlined in Scheme 1.[9–11]

Analogues **37–40** were intended as tryprostatin A mimics in which the alkyl substituent was moved from the indole 2-position to the indole NH. This was expected to result in analogues that are more readily accessible than the natural products which require methods for prenylation of tryptophan at C-2. As shown in Scheme 2, the *ortho*-iodoaniline **26** was coupled with the internal alkyne[10] **27** in the presence of catalytic $Pd(OAc)_2$ with Na_2CO_3 as the base to provide indole **28** in 77% yield.[45,46]

Alkylation of **28** with methyl iodide, isoprenyl bromide, benzyl bromide or allyl bromide in the presence of sodium hydride afforded the indole N_a-substituted analogues **29–32** in 72–99% yields. Hydrolysis of pyrazines **29–32** with 2 N aq HCl in THF resulted in removal of both the bislactim ether moiety and the silyl group. Tryptophans **33–36** were readily transformed into analogues **37–40** of tryprostatin A under conditions analogous to the steps in Scheme 1.

In order to synthesize the N_a-substituted analogues (**46** and **47**) of **1**, in region B in which the indole 2-position carried the isoprenyl group, an analogous strategy was employed. Thermal removal of the Boc protecting group of **16** (Scheme 3) in refluxing xylene afforded pyrazine **41**. Alkylation of **41** with benzyl bromide or allyl bromide using sodium hydride afforded analogues **42** and **43** in 91% and 82% yields, respectively. These intermediates were readily transformed into analogues **46** and **47** of tryprostatin A under conditions analogous to the steps in Scheme 1, as illustrated in Scheme 3.

To obtain analogues with different substitution at the indole 2-position (region C) of **1**, 2-bromo-indole **48** (Scheme 4) served as a common intermediate which was easily obtained from indole **28** after sequential treatment with NBS and Boc anhydride. As shown in Scheme 4, lithium–halogen exchange, followed by treatment with benzyl bromide or allyl bromide furnished the 2-substituted analogues **49** and **50**. Analogues **49** and **50** were further transformed into 2-substituted indoles **55** and **56**, respectively, under standard conditions (Scheme 4). For the synthesis of **51** (Scheme 4), the zinc reagent was prepared through lithium–halogen exchange followed by treatment with zinc chloride. Negishi coupling[47] of the zinc reagent with phenyl iodide using $Pd(OAc)_2$ in the presence of trifuryl phosphine afforded the 2-phenyl indole **51** in 65% yield which was then transformed to analogue **57** under conditions outlined in Scheme 4. A variety of other conditions were attempted to prepare the 2-phenyl indole **51**, however the Negishi coupling was the only method that was successful in a practical sense.

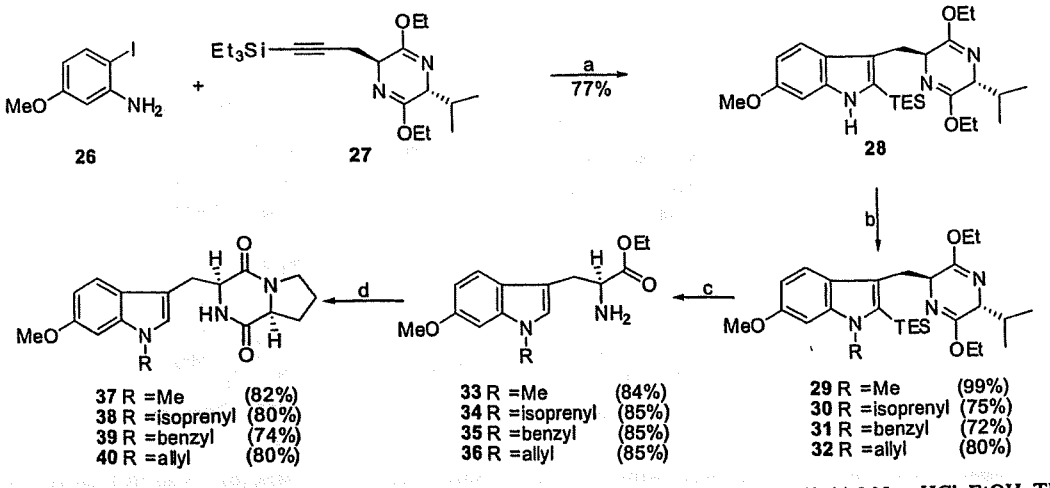

Scheme 2. Reagents and conditions: (a) $Pd(OAc)_2$, LiCl, Na_2CO_3, DMF, 100 °C, 77%; (b) NaH, DMF, RX; (c) 2 N aq HCl, EtOH, THF, −78 °C to rt; (d) **24**, TEA, $CHCl_3$; DEA, CH_3CN, rt; xylene, reflux.

Heck coupling[48] of bromide **48** with methyl acrylate in the presence of 5% $Pd(PPh_3)_4$ and Cy_2NEt afforded the coupled product **58** in 94% yield (Scheme 5). Analogue **58** (Scheme 5) was then transformed into ester

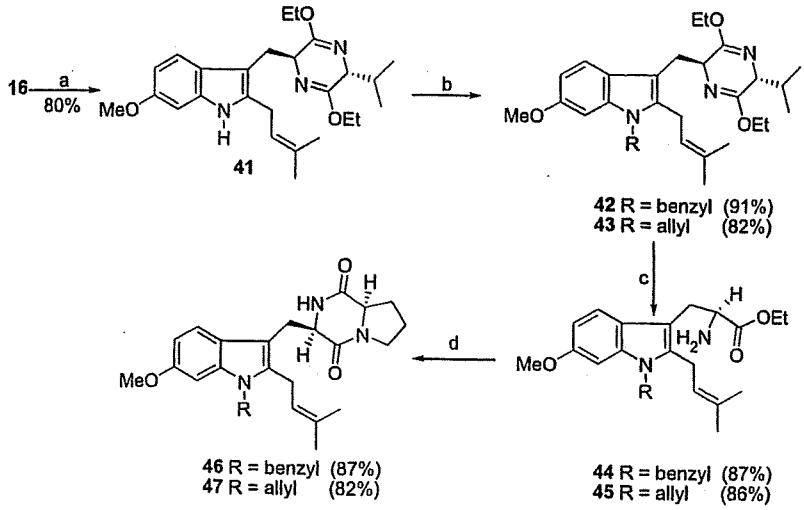

Scheme 3. Reagents and conditions: (a) xylene, reflux, 80%; (b) NaH, DMF, RX; (c) 2 N aq HCl, EtOH, THF, −78 °C to rt; (d) **24**, TEA, $CHCl_3$; DEA, CH_3CN, rt; xylene, reflux.

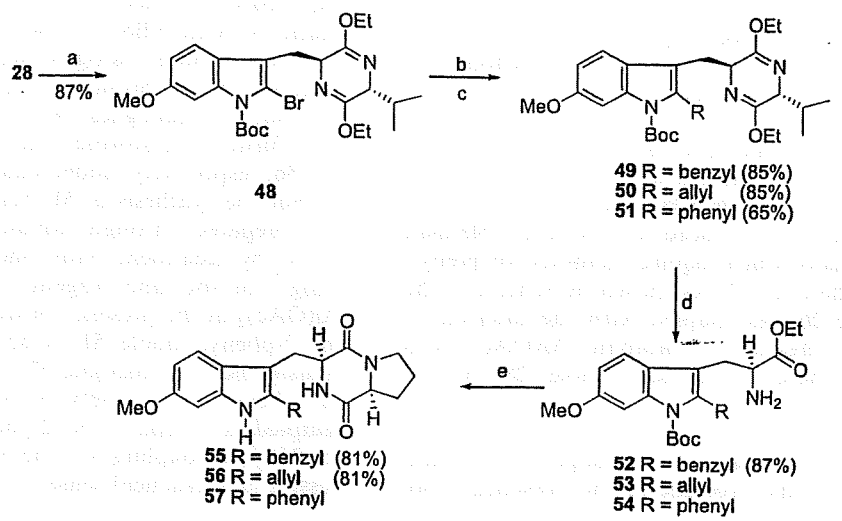

Scheme 4. Reagents and conditions: (a) NBS, CH_3CN; $(Boc)_2O$, DMAP, CH_3CN, rt, 87%; (b) *n*-BuLi, THF, −78 °C; RX; (c) *n*-BuLi, THF, −78 °C; $ZnCl_2$; $Pd(OAc)_2$, PhI, tri-2-furyl phosphine, rt, 65%; (d) 2 N aq HCl, EtOH, THF, −78 °C to rt; (e) **24**, TEA, $CHCl_3$; DEA, CH_3CN, rt; xylene, reflux.

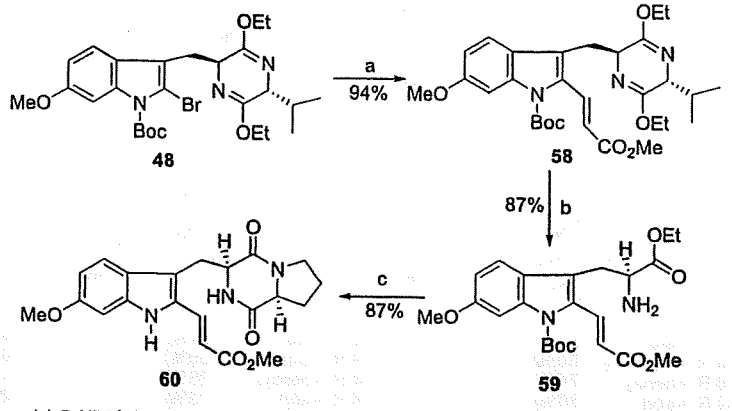

Scheme 5. Reagents and conditions: (a) $Pd(PPh_3)_4$, methyl acrylate, Cy_2NMe, toluene, 95 °C, 94%; (b) 2 N aq HCl, EtOH, THF, −78 °C to rt, 80%; (c) **24**, TEA, $CHCl_3$; DEA, CH_3CN, rt; xylene, reflux.

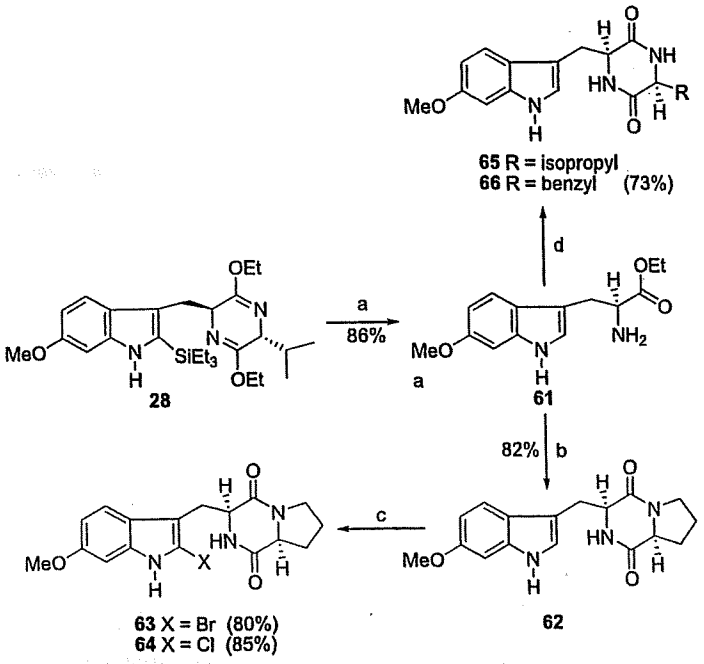

Scheme 6. Reagents and conditions: (a) 2 N aq HCl, EtOH, THF, −78 °C to rt, 86%; (b) **24**, TEA, $CHCl_3$, DEA, CH_3CN, rt; xylene, reflux; (c) NBS or NCS, THF, −78 °C to rt; (d) Fmoc-L-amino-acyl chloride, TEA, $CHCl_3$; DEA, CH_3CN, rt; xylene, reflux.

60, analogous to well-developed processes outlined previously in Scheme 1. It was well known in the literature that the 6-methoxy group activated the C-2 position of the indole nucleus towards electrophilic substitution. As illustrated in Scheme 6, indole **28** was hydrolyzed with aq 2 N HCl to afford the 6-methoxy-L-tryptophan ethyl ester **61** in 86% yield. Ester **61** was further transformed into the N_a–H analogue **62** under conditions similar to that described for **1** in Scheme 1. Analogue **62** was treated with NBS at −78 °C to afford 2-bromo-indole **63** in 80% yield. The corresponding 2-chloro analogue **64** was prepared in 85% yield (from NCS) under analogous conditions to those described above for the preparation of 2-bromo-indole **63**.

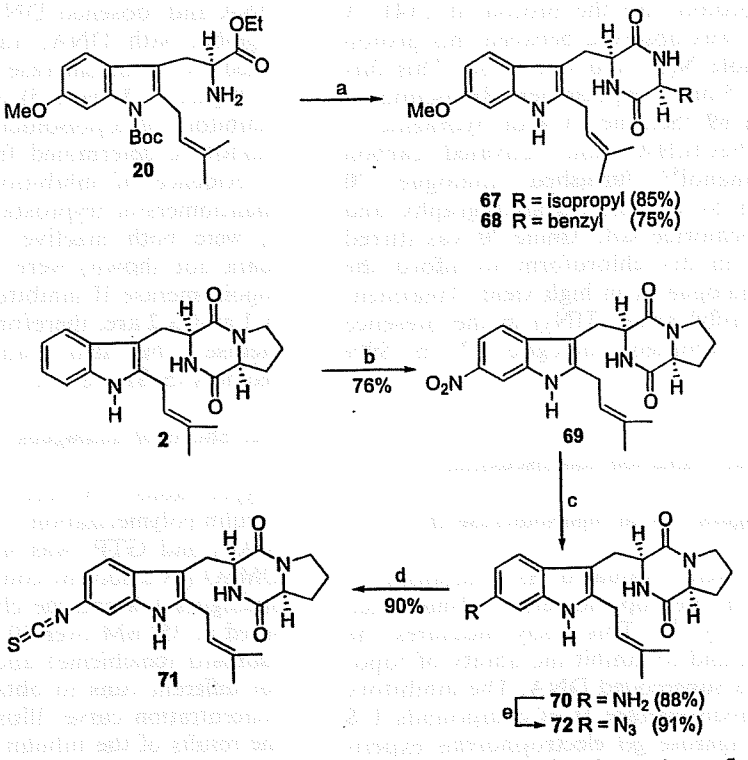

Scheme 7. Reagents and conditions: (a) Fmoc-L-amino-acylchloride, TEA, $CHCl_3$; DEA, CH_3CN, rt; xylene, reflux; (b) $NaNO_2$, TFA, −78 °C to −20 °C, 75%; (c) NH_2NH_2, $FeCl_3.6H_2O$, active C, MeOH, reflux, 91%; (d) $CHCl_3$, ClC(S)Cl, 93%; (e) TfN_3, aq $CuSO_4$, Et_3N, CH_2Cl_2/MeOH, 89%.